

# Soft-TransFormers for Continual Learning

**Haeyong Kang**

HAEYONG.KANG@KAIST.AC.KR

*School of Electrical Engineering (EE)*

*Korea Advanced Institute of Science and Technology (KAIST)*

*291 Daehak-ro, Yuseong-gu, Daejeon 34141, Republic of Korea*

**Chang D. Yoo**

CD\_YOO@KAIST.AC.KR

*School of Electrical Engineering (EE)*

*Korea Advanced Institute of Science and Technology (KAIST)*

*291 Daehak-ro, Yuseong-gu, Daejeon 34141, Republic of Korea*

## Abstract

Inspired by *Well-initialized Lottery Ticket Hypothesis (WLTH)*, which provides suboptimal fine-tuning solutions, we propose a novel fully fine-tuned continual learning (CL) method referred to as Soft-TransFormers (Soft-TF). Soft-TF sequentially learns and selects an optimal soft-network for each task. During sequential training in CL, an well-initialized Soft-TF mask optimizes the weights of sparse layers to obtain task-adaptive soft (real-valued) networks, while keeping the well-pre-trained layer parameters frozen. In inference, the identified task-adaptive network of Soft-TF masks the parameters of the pre-trained network, mapping to an optimal solution for each task and minimizing Catastrophic Forgetting (CF) - the soft-masking preserves the knowledge of the pre-trained network. Extensive experiments on the Vision Transformer (ViT) and the Language Transformer (Bert) demonstrate the effectiveness of Soft-TF, achieving state-of-the-art performance across Vision and Language Class Incremental Learning (CIL) scenarios.

**Keywords:** Continual Learning (CL), Soft-TransFormers (Soft-TF), Adapter, and LoRA.

## 1 Introduction

Continual Learning (CL), also known as Lifelong Learning (Thrun, 1995; Rusu et al., 2016; Zenke et al., 2017; Hassabis et al., 2017), is a learning paradigm where a series of tasks are learned sequentially. The principle objective of continual learning is to replicate human cognition, characterized by the ability to learn new concepts incrementally throughout one’s lifespan. An optimal continual learning system could facilitate a positive forward and backward transfer, leveraging the knowledge gained from previous tasks to solve new ones, while also updating its understanding of previous tasks with the new knowledge. However, achieving continual learning is challenging due to the occurrence of *catastrophic forgetting* or *catastrophic interference* (McCloskey and Cohen, 1989), a phenomenon where the performance of the model on previous tasks deteriorates significantly when it learns new tasks. This can make it challenging to retain the knowledge acquired from previous tasks, ultimately leading to a decrease in overall performance. To address the issue of catastrophic forgetting during continual learning, numerous conventional approaches have been proposed on Convolutional Neural Networks (CNNs), which can be broadly classified as follows: (1) **Regularization-based methods** (Kirkpatrick et al., 2017; Chaudhry et al., 2020; Jung et al., 2020; Titsias et al., 2020; Mirzadeh et al., 2021) aim to keep the learned information of

past tasks during continual training aided by sophisticatedly designed regularization terms, (2) **Rehearsal-based methods** (Rebuffi et al., 2017; Riemer et al., 2018; Chaudhry et al., 2019a,b; Saha et al., 2021) utilize a set of real or synthesized data from the previous tasks and revisit them, and (3) **Architecture-based methods** (Mallya et al., 2018; Serrà et al., 2018; Li et al., 2019; Wortsman et al., 2020; Kang et al., 2022, 2023, 2024a) propose to minimize the inter-task interference via newly designed architectural components.

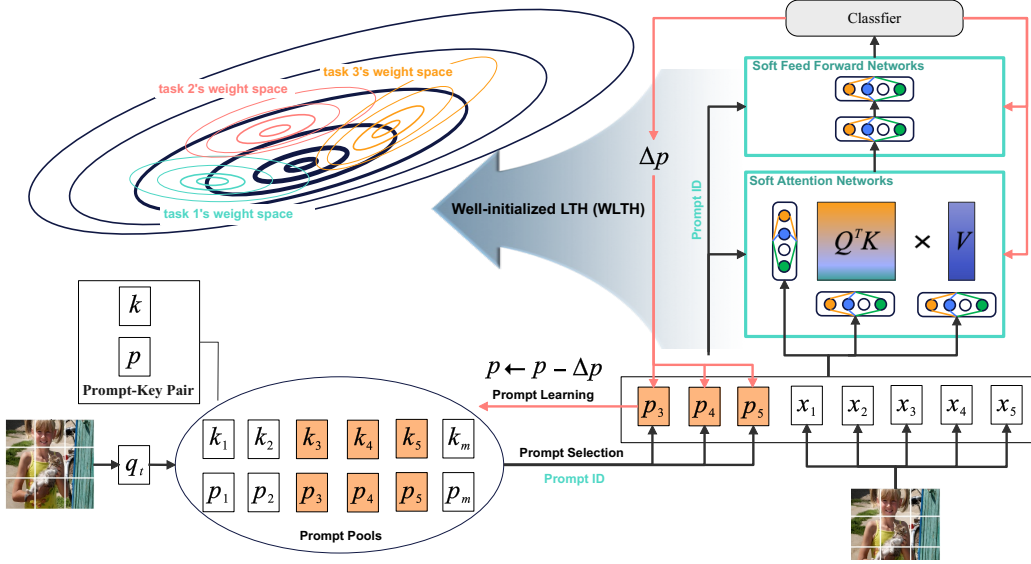


Figure 1: **Soft-TransFormers (Soft-TF)**: the objective is to design a fully fine-tuned model that works well across multiple continual learning settings with incurring task-wise soft network training of attention and feedforward networks, leveraged by WLTH.

Developing neural network models that leverage large-scaled pre-trained models. i.e., Vision Transformer (ViT) (Dosovitskiy et al., 2020) and Contrastive Language-Image Pre-training (CLIP) (Radford et al., 2021) leads to a new paradigm shift referred to as (4) **Prompt-based methods** in Continual Learning (CL). Prompt-based methods learn continual representations to provide fixed pre-trained transformers with additional instruction. Notably, while L2P (Wang et al., 2022c) stands out as the seminal work that bridges the gap between prompting and continual learning, DualPrompt (Wang et al., 2022b) introduces an innovative approach to affixing complementary prompts to the pre-trained backbone, thereby enabling the acquisition of both task-invariant and task-specific instructions. Additionally, other notable contributions in this field encompass DyTox (Douillard et al., 2022), S-Prompt (Wang et al., 2022a), CODA-P (Smith et al., 2023b), ConStruct-VL (Smith et al., 2023a), ST-Prompt (Pei et al., 2023), and LGCL (Khan et al., 2023). Recently, Qiao et al. (2024) investigated prompt-projection for better generalized continual learners.

With prior developments of representational research, current prompt-based models can be fine-tuned using trainable prompts to improve their performance on sequential tasks, and the fixed pre-trained backbone can consistently provide unforgettable base session knowledge. However, prompt-based models come with several disadvantages and limitations. First, the prompt-based CL model is highly dependent on the quality and design of the sample or the

task-relevant prompts. Poorly trained prompts could lead to suboptimal performance or tend to be biased. Second, managing and maintaining a large set of prompts can become cumbersome and unmanageable as the number of tasks increases. Lastly, prompt tuning is not as flexible as full fine-tuning. The only prompt-tuning with the pre-trained model cannot capture all the nuances of uncorrelated sequential tasks even though leveraging the frozen well-initialized model pre-trained on large-scale datasets since the only frozen well-initialized model provides global solutions rather than task-specific solutions. These disadvantages motivate us to make informed decisions about when and how to use prompt-based models and explore alternative methods like full fine-tuning for more robust and flexible prompt-based continual learning performance.

To overcome the limitations of conventional prompt-based methods, the central focus of this work is to pinpoint the parameter-efficient fine-tuning representations of frozen pre-trained networks, comparing with conventional LLM-based fine-tuning methods such as Adapter (Houlsby et al., 2019) and LoRA (Hu et al., 2021), as shown in Figure 2. We focus on two main issues when sequentially fine-tuning the pre-trained foundation models: (1) Catastrophic Forgetting (CF) and (2) parameter-efficient fine-tuning CL model. To deploy a practical model to deal with the two points, we suggest a new paradigm for Continual Learning (CL), named *Well-initialized Lottery Ticket Hypothesis*:

**Well-initialized Lottery Ticket Hypothesis (WLTH).** *A well-initialized dense neural network contains globally minimal solutions that can retain the prior class knowledge while providing room to learn the new class knowledge through isolated fine-tuning of the networks or subnetworks.*

Leveraged by the WLTH, this work proposes a new Soft-Transformer (Soft-TF) to address fine-tuning with minimal CF, as shown in Figure 1. In this work, we find task-specific soft-networks based on well-trained frozen transformer parameters that incrementally learn task-adaptive weights associated with sequential tasks.

Our contributions can be summarized as follows:

- Inspired by *Well-initialized Lottery Ticket Hypothesis (WLTH)*, we propose a novel continual learning method referred to as Soft-Transformers (Soft-TF), which learns compact task-specific soft-networks from well pre-trained parameters for each task.
- Extensive experiments demonstrate that Soft-TF leads to better generalized parameter-efficient continual models than baselines such as DualPrompts, Adaptor, and LoRA, achieving state-of-the-art performances on Vision and Language Class-Incremental Learning (CIL) scenarios.

## 2 Related Works

**Continual Learning** (McCloskey and Cohen, 1989; Thrun, 1995; Kumar and Daume III, 2012; Li and Hoiem, 2016) is the challenge of learning a sequence of tasks continuously while utilizing and preserving previously learned knowledge to improve performance on new tasks. Four major approaches have been proposed to tackle the challenges of continual learning, such as catastrophic forgetting. One such approach is (1) *Regularization-based approaches* (Kirkpatrick et al., 2017; Chaudhry et al., 2020; Jung et al., 2020; Titsias et al.,

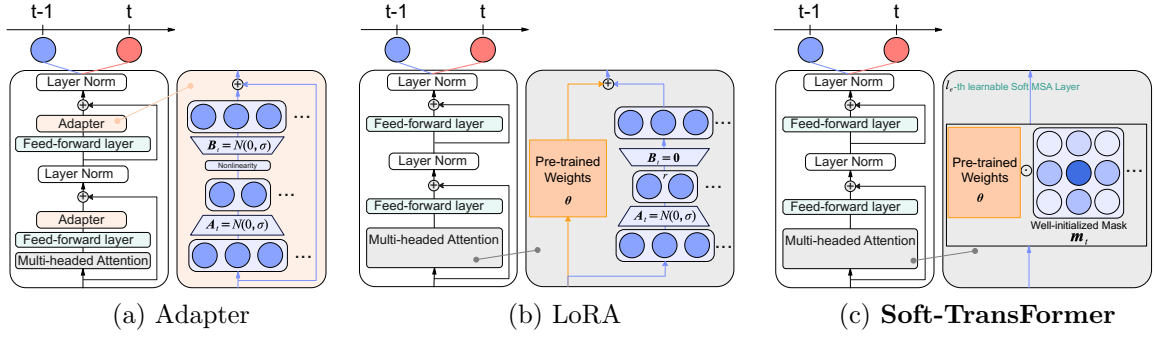


Figure 2: **Comparisons of LLM-based fine-tuning methods (Adapters, LoRA) with Soft-TransFormer (Soft-TF)**: well-initialized Soft-TF  $\theta \odot m_t$  is trained at  $l_e$ -th or only few attention layers while LLM fine-tuning methods such as Adapter (Houlsby et al., 2019) and LoRA (Hu et al., 2021) are trained at all attention layers. Note that all pre-trained parameters  $\theta$  are fixed in fine-tuning  $t$ -th task parameter  $m_t$  in Continual Learning (CL) scenarios.

2020; Mirzadeh et al., 2021), which aim to reduce catastrophic forgetting by imposing regularization constraints that inhibit changes to the weights or nodes associated with past tasks. (2) *Rehearsal-based approaches* (Rebuffi et al., 2017; Chaudhry et al., 2019a,b; Saha et al., 2021; Deng et al., 2021; Sun et al., 2023; Sarfraz et al., 2023; Mai et al., 2021; Lin et al., 2023; Aljundi et al., 2019; Caccia et al., 2021; Chaudhry et al., 2019c; Liang and Li, 2024; Buzzega et al., 2020) store small data summaries to the past tasks and replay them during training to retain the acquired knowledge. Some approaches in this line of work (Shin et al., 2017; Aljundi et al., 2019) accommodate the generative model to construct the pseudo-rehearsals for previous tasks. (3) *Architecture-based approaches* (Mallya et al., 2018; Serrà et al., 2018; Li et al., 2019; Wortsman et al., 2020; Kang et al., 2022, 2023, 2024b,a) use the additional capacity to expand (Xu and Zhu, 2018), dynamic representation (Yan et al., 2021; Singh et al., 2020) or isolate (Rusu et al., 2016) model parameters, preserving learned knowledge and preventing forgetting. Rehearsal and architecture-based methods have shown remarkable efficacy in suppressing catastrophic forgetting but require additional capacity for the task-adaptive parameters (Wortsman et al., 2020) or the replay buffers. Recently, (4) *Prompt-based approaches*, an emerging transfer learning technique, harnesses a fixed function of pre-trained Transformer models. This empowers the language model to receive additional instructions for enhancing its performance on downstream tasks. Two key works stand out in the prompt-based CL: L2P (Wang et al., 2022c), a seminal study bridging the gap between prompting and continual learning, and DualPrompt (Wang et al., 2022b), which proposes an innovative method for attaching complementary prompts to a fixed pre-trained backbone. Here, for the first time, we introduce a new approach to update the fixed pre-trained parameters through learnable sparse layered soft-networks under the convergence theory, maximumly enabling the acquisition of task-invariant and task-specific instructions with prompts.

**Prompt-based CL.** With advances in Vision Transformers (Khan et al., 2022) and prompt-based fine-tuning in NLP (Li and Liang, 2021) and CL (Razdaibiedina et al., 2023), Wang et al. (2022c) have shown that interacting with a pre-trained model via prompt learning

is a promising approach, L2P (Wang et al., 2022c) for continual learning. Then, other advanced prompt-based CL models emerged such as DualPrompt (Wang et al., 2022b), DyTox (Douillard et al., 2022), S-Prompt (Wang et al., 2022a), CODA-P (Smith et al., 2023b), ConStruct-VL (Smith et al., 2023a), ST-Prompt (Pei et al., 2023), and LGCL (Khan et al., 2023). Recently, Prompt Gradient Projection (PGP) (Qiao et al., 2024), a small set of learnable orthogonal parameters, is appended to the input and enables quick adaptation of a frozen ImageNet pre-trained model to new streaming tasks. Their analysis shows that directly leveraging the pre-trained vision-language model without introducing any learnable parameters is a simple yet promising approach to continual learning. The PGP was also adopted to a joint vision-language model like CLIP (Radford et al., 2021) for continual learning, which presents multiple advantages - catering to practical scenarios without well-defined task identities and boundaries in class incremental learning scenarios. However, prompt-based models come with several disadvantages. Poorly trained prompts could lead to suboptimal performance or tend to be biased. Moreover, prompt tuning could not capture all nuances of uncorrelated sequential tasks. These disadvantages lead to exploring alternative methods like full fine-tuning or hybrid approaches for more robust and flexible prompt-based model performance. In this work, to alleviate these issues of prompt tuning, we investigate a fully fine-tuning of well-pre-trained transformers on training soft networks on various continual learning scenarios, comparing with LLM-based CL baselines such as MBPA++ (de Masson D’Autume et al., 2019), IDBR (Huang et al., 2021), and SLM (Bohao et al., 2024).

### 3 Prerequisites

We start with conventional prompt-based continual learning methods using Vision Transformer (ViT) (Dosovitskiy et al., 2020) in Class Incremental Learning (CIL) scenarios.

#### 3.1 Problem Statement

Continual Learning (CL) involves training deep neural networks (DNN) on time-variant data represented as a sequence of tasks,  $\mathcal{D} = \{\mathcal{D}_1, \dots, \mathcal{D}_T\}$ . Each  $t$ -th task,  $\mathcal{D}_t = \{(\mathbf{x}_i^t, y_i^t)_{i=1}^{n_t}\}$  consists of  $n_t$  tuples where  $\mathbf{x}_i^t \in \mathcal{X}_t$  is an input sample and  $y_i^t \in \mathcal{Y}_t$  is the corresponding label. When a task  $\mathcal{X}_t$  arrives, a model  $f_\theta$  is trained for the current task, while data from previous tasks is inaccessible. This work focuses primarily on class incremental learning (CIL), in which the task-ID is not given during inference.

#### 3.2 Prompt-based Class Incremental Learning (CIL)

A simple yet effective prompt-based (prompt-tuning) CIL model: Learning to Prompt (L2P) (Wang et al., 2022c) is first proposed. In this model, a prompt  $p$ , a tiny set of trainable tokens combined with image features, is fed into the Vision Transformer (ViT) to help the model resist forgetting. To select suitable prompts for task-specific training, L2P utilizes a prompt pool  $P$  containing numerous prompt-key pairs,  $\{p_t, k_t\}_{t=1}^T$ , where  $p_t \in \mathbb{R}^{1 \times D}$  represents the  $t$ -th task prompt,  $k_t$  represents the  $t$ -th corresponding task key, and  $T$  is the total number of prompt-key pairs. Building on L2P, DualPrompt (Wang et al., 2022b) divided the prompts into expert (**E**-) prompts and general (**G**-) prompts for distinct

features learning. DualPrompt also replaced prompt-tuning with prefix-tuning, which was successfully proven in Language CIL scenarios.

## 4 Transformer with Learnable Soft-networks

In this section, we explain how Soft-TransFormers (Soft-TF) leverage learnable soft-networks to train sequential tasks while keeping the well-pretrained model parameters fixed. To introduce our novel Soft-TF and provide a clearer understanding, we draw on a partial explanation of DualPrompt.

### 4.1 Soft-MSA Layers

To address the task-specific fine-tuning of the pre-trained model, such as ViT, this work proposes a new Soft-Transformer (Soft-TF), as illustrated in Figure 1. The proposed Soft-TF consists of a conventional neural network, like a multilayer transformer with multihead attention and forward networks. Using well-trained transformer parameters, we could discover task-specific soft-networks, as depicted in Figure 4. The Soft-TF incrementally learns model weights and task-adaptive soft-masks with well-pre-trained and soft-network parameters  $\mathbf{m}$ .

The Soft-TF originates from learned parameters distributed with  $\mu \approx 1.0$  & various variances, as stated in Figure 3: the histogram density plots compare the distribution of parameters for the attention layer L[12] in two contexts: the masking mechanism ( $\mathbf{m}^{QKV}$ ) and the fine-tuned weighted product ( $\mathbf{w}^{QKV} \odot \mathbf{m}^{QKV}$ ) for two tasks (Task 2 and Task 3). In Figure 3(a), the  $\mathbf{m}^{QKV}$  parameters are concentrated in a narrow range centered around 1. There is a slight variation between Task 2 and Task 3. However, the overall range remains consistent.  $\mathbf{m}^{QKV}$  acts as a soft gating mechanism, controlling which pre-trained parameters are retained or modified during fine-tuning. In Figure 3(b), the distribution of pre-trained weight ( $\mathbf{w}^{QKV}$ ) is centered around 0, with a Gaussian-like spread. The distribution of soft-masked fine-tuned weight ( $\mathbf{w}^{QKV} \odot \mathbf{m}^{QKV}$ ) remain similar to that of  $\mathbf{w}^{QKV}$  but slightly narrower. The overlap between the two distributions indicates that the fine-tuning process maintains the general structure of the pre-trained weights while introducing task-specific modifications. By using soft-masks  $\mathbf{m}^{QKV}$ , Soft-TF ensures task-specific fine-tuning, reducing the risk of catastrophic forgetting and improving performance in various sequential tasks. The task-specific Soft-TF fine-tuning enables the models to infer task ID ideally in following Vision CIL scenarios.

Given a pre-trained parameter  $\boldsymbol{\theta}$  and learnable soft-parameters  $\mathbf{m}$ , Soft-ViT is represented as  $f_{\boldsymbol{\theta} \odot \mathbf{m}}$ , consisting of  $N$  consecutive soft-MSA layers. We extend the notation by denoting the input embedding feature of the  $l_*$ -th learnable soft-MSA layer as  $\mathbf{h}^{(l_*)}$ , where  $l_* = 1, 2, \dots, N$ , and  $l_*$  can refer to either the G-Prompt layer  $l_g$  or the E-Prompt layer  $l_e$ . Note that while the pre-trained parameters  $\boldsymbol{\theta}$  remain fixed, the soft-parameters  $\mathbf{m}$  are updated to provide task-specific solutions.

**G-prompt.**  $\mathbf{g} \in \mathbb{R}^{L_g \times D}$  with sequence length  $L_g$  and embedding dimension  $D$ , is a shared parameter for all tasks. G-Prompt is attached to the  $l_g$ -th MSA layer to transform  $\mathbf{h}^{(l_g)}$  via a prompting function as follows:

$$\mathbf{h}_g^{(l_g)} = f_{\boldsymbol{\theta}}^{\text{prompt}}(\mathbf{g}, \mathbf{h}^{(l_g)}), \quad (1)$$



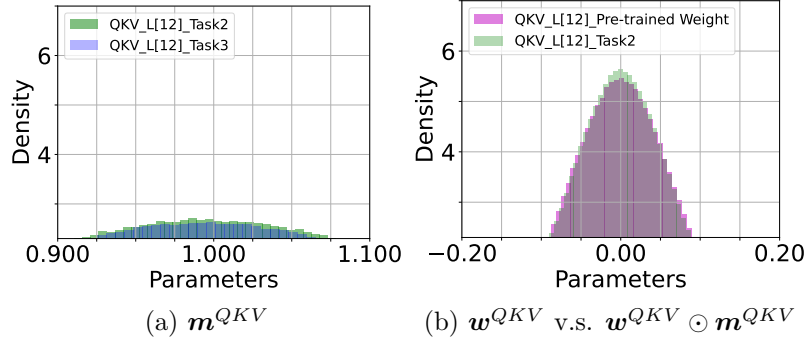


Figure 3: **Attention Layer-(L[12]) Histogram Density Estimates** of Pre-trained weight ( $\theta$ ) and Soft-TF ( $m$ ) on 10-Split-CIFAR100.

where  $f_{\theta}^{prompt}$  defines the approach for attaching the prompt to the hidden embeddings.

**E-prompt & Soft-networks.**  $e = \{e_t\}_{t=1}^{\mathcal{T}}$  is a set of task-dependent parameters, where  $e_t \in \mathbb{R}^{L_e \times D}$  has as sequence length of  $L_e$  and the same embedding dimension  $D$  as the G-prompt, and  $\mathcal{T}$  is the total number of tasks. Unlike the shared G-prompt, each  $e_t$  is associated with a task-specific key  $k_t \in \mathbb{R}^D$ , which is also a learnable parameter aimed at capturing representative features of a task. For an input example from the  $t$ -th task, to attach E-prompt to the  $l_e$ -th soft-MSA layer, we apply the prompting function in a similar way:

$$h_e^{(l_e)} = f_{\theta \odot m}^{prompt}(e_t, h^{(l_e)}). \quad (2)$$

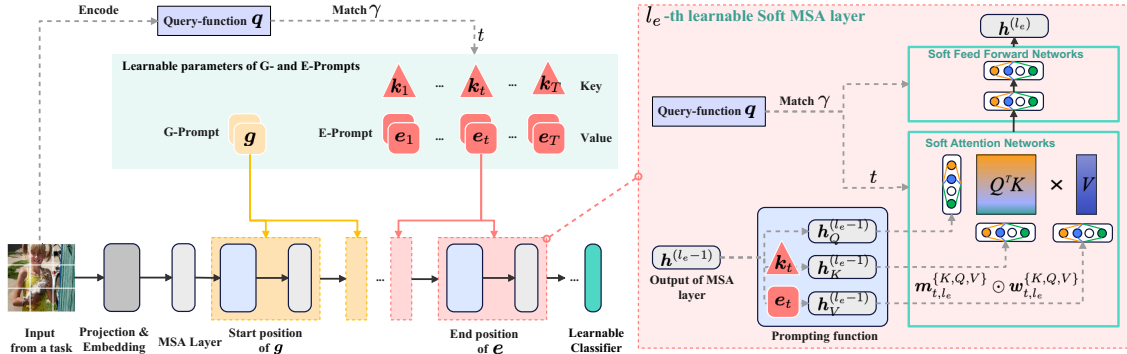


Figure 4: **Soft-TransFormers (Soft-TF)**: At training time, the E-Prompt and the Soft-network are selected according to task identity, and the selected G-Prompt, E-Prompt, and the Soft-networks (Soft-Attention and Feed Forwards) are trained together with a classifier. At test time, an input is transformed by a query function (Prompt ID) or task identifier (Gradient ID) to match the closest task key  $k_t$ , E-prompt  $e_t$  and Soft-networks  $m_t^{\{K,Q,V\}}$ . Note task identifier is depicted in Section 5.

## 4.2 Prompts with Learnable Subnetworks

G- and E-prompts, along with learnable soft-networks, encode specific types of instructions during training with the backbone and work together to guide the model’s predictions during inference. We have demonstrated the method for attaching prompts and learnable soft-networks to a single soft-MSA layer. Similarly to the approach taken in DualPrompt (Wang et al., 2022b), we also investigate layers of E-prompts with learnable soft-networks  $\mathbf{m}$ , while utilizing the layers designated for G-prompts.

**Layers of G- and E-Prompts.** We use the multilayered extension of both types of prompts:  $\mathbf{g} = \{\mathbf{g}^{(l_g)}\}_{l_g=start_g}^{end_g}$ , where  $\mathbf{g}^{(l_g)} \in \mathbb{R}^{L_g \times D}$  represents the G-prompt attached to the  $l_g$ -th MSA layer. Similarly, we define  $\mathbf{e}_t = \{\mathbf{e}_t^{(l_e)}\}_{l_e=start_e}^{end_e}$  for the  $l_e$ -th conventional MSA layer. In this configuration, the G-prompt  $\mathbf{g}^{(l_g)}$  is attached from the  $start_g$ -th to the  $end_g$ -th conventional MSA layers, and the E-prompt  $\mathbf{e}_t^{(l_e)}$  is attached to the  $[start_e, end_e]$ -th soft-MSA layers, ensuring that there is no overlap between them. In our experiments, we follow the  $l_g \notin [start_e, end_e]$  ( $l_g = [1, 2]$ ) settings used in DualPrompt and empirically search for the optimal  $[start_e, end_e]$  layers for the learnable subnetworks through ablation studies.

**Learnable Soft-networks.** The prompting function  $f_{\theta \odot \mathbf{m}}^{prompt}$  determines how prompts ( $\mathbf{p}$ ) are combined with fine-tuned soft ( $\theta \odot \mathbf{m}$ ) embedding features. From another perspective,  $f_{\theta \odot \mathbf{m}}^{prompt}$  directly influences the interaction between high-level instructions in the prompts and low-level representations. Therefore, we believe that a well-designed prompting function, along with task-specific parameters, is crucial for optimizing overall continual learning performance.

Specifically, applying a prompting and fine-tuning function  $f_{\theta \odot \mathbf{m}}^{prompt}$  can be seen as modifying the inputs to the soft-MSA layers. Let the input to the soft-MSA layer be  $\mathbf{h} \in \mathbb{R}^{L \times D}$ , and denote the input query, key, and values for the soft-MSA layer as  $\mathbf{h}_Q$ ,  $\mathbf{h}_K$ , and  $\mathbf{h}_V$ , respectively. A soft-MSA layer is defined by the following equation:

$$\text{MSA}(\mathbf{h}_Q, \mathbf{h}_K, \mathbf{h}_V) = [\mathbf{h}_1, \dots, \mathbf{h}_i, \dots, \mathbf{h}_n] \mathbf{w}^O \odot \mathbf{m}^O \quad (3)$$

where  $\mathbf{h}_i = \text{Attention}(\mathbf{h}_Q(\mathbf{w}_i^Q \odot \mathbf{m}^Q), \mathbf{h}_K(\mathbf{w}_i^K \odot \mathbf{m}^K), \mathbf{h}_V(\mathbf{w}_i^V \odot \mathbf{m}^V))$ ;  $\mathbf{w}_i^O, \mathbf{w}_i^Q, \mathbf{w}_i^K$ , and  $\mathbf{w}_i^V$  are fixed projection matrices while  $\mathbf{m}^O, \mathbf{m}^Q, \mathbf{m}^K$ , and  $\mathbf{m}^V$  are learnable parameters.  $s$  is the number of heads. In ViT,  $\mathbf{h}_Q = \mathbf{h}_K = \mathbf{h}_V$ . Here, we define a unified prompt parameter with a sequence length of  $L_p$ , such as  $\mathbf{p} \in \mathbb{R}^{L_p \times D}$  for a single-layered G- or E-prompt.

## 4.3 Fine-tuning on Well-initialized Parameters

In this framework, we concatenate the prompts  $\mathbf{p}_t$  and the embedding sequence  $\mathbf{x}_t$ , i.e., inputs from  $t$ -th task, along the embedding dimension:  $\mathbf{z}_t = [\mathbf{p}_t; \mathbf{x}_t]$ . With the weights of  $\mathbf{w}^Q \odot \mathbf{m}^Q, \mathbf{w}^K \odot \mathbf{m}^K, \mathbf{w}^V \odot \mathbf{m}^V$ , the soft-transformer takes query ( $\mathbf{q}_t = (\mathbf{w}^Q \odot \mathbf{m}^Q) \mathbf{z}_t$ ) and key ( $\mathbf{k}_t = (\mathbf{w}^K \odot \mathbf{m}^K) \mathbf{z}_t$ ) as input of the soft-MSA layer. The soft-attention matrix is then given by:

$$\mathbf{a}_t = \text{softmax} \left( \frac{\mathbf{q}_t \mathbf{k}_t^T}{\sqrt{D/n}} \right) \quad (4)$$



where we focus on  $\mathbf{q}_t \mathbf{k}_t^T = (\mathbf{w}^Q \odot \mathbf{m}^Q) \mathbf{z}_t$  and  $\mathbf{z}_t^T (\mathbf{w}^K \odot \mathbf{m}^K)^T$ . First, the trainable prompt parameters can be denoted as:

$$\mathbf{z}_t \cdot \mathbf{z}_t^T = \begin{bmatrix} \mathbf{p}_t \\ \mathbf{x}_t \end{bmatrix} \begin{bmatrix} \mathbf{p}_t & \mathbf{x}_t \end{bmatrix} = \begin{bmatrix} \mathbf{p}_t \mathbf{p}_t^T & \mathbf{p}_t \mathbf{x}_t^T \\ \mathbf{x}_t \mathbf{p}_t^T & \mathbf{x}_t \mathbf{x}_t^T \end{bmatrix} \quad (5)$$

Second, the trainable soft-attention layer’s parameters with  $\mathbf{m}^Q$  and  $\mathbf{m}^K$  are as follows:

$$\begin{Bmatrix} \mathbf{m}^Q \cdot \mathbf{p}_t \mathbf{p}_t^T \cdot (\mathbf{m}^K)^T, \\ \mathbf{m}^Q \cdot \mathbf{x}_t \mathbf{p}_t^T \cdot (\mathbf{m}^K)^T, \\ \mathbf{m}^Q \cdot \mathbf{p}_t \mathbf{x}_t^T \cdot (\mathbf{m}^K)^T, \\ \mathbf{m}^Q \cdot \mathbf{x}_t \mathbf{x}_t^T \cdot (\mathbf{m}^K)^T. \end{Bmatrix} \quad (6)$$

where  $\mathbf{w}^Q$  and  $\mathbf{w}^K$  are frozen and unchanged during training and test. The trainable soft-attention layer’s parameters  $\mathbf{m}^*$  are used to analyze the convergence rate of the Soft-Transformer (see [Appendix A.1](#) stated in detail).

#### 4.4 Optimization of Soft-Transformers

The overall process of the Soft-Transformers (Soft-TF) during training and testing is described as [Algorithm 1](#) and [Algorithm 2](#). We denote the architecture with attached prompts as  $f_{g,e_t,m_t}$ . The input  $\mathbf{x}$  of the  $t$ -th task is transformed using  $f_{g,e_t,m_t}$  and then passed to the classification head  $f_\phi$ , parameterized by  $\phi$ , for prediction. Finally, we train the two prompts, the task keys, the soft-attention parameters, and the newly-initialized classification head in an end-to-end manner:

$$\min_{g,e_t,m_t,k_t,\phi} \mathcal{L}(f_\phi(f_{g,e_t,m_t}(\mathbf{x})), y) + \lambda \mathcal{L}_{\text{match}}(\mathbf{x}, \mathbf{k}_t), \quad (7)$$

Here,  $\mathcal{L}$  represents the cross-entropy loss, and  $\mathcal{L}_{\text{match}}(\mathbf{x}, \mathbf{k}_t) = \gamma(\mathbf{q}(\mathbf{x}), \mathbf{k}_t)$  denotes the matching loss, where  $\mathbf{q}(\mathbf{x}) = f(\mathbf{x})[0]$  corresponds to the feature vector associated with the [class] token ([Dosovitskiy et al., 2020](#); [Wang et al., 2022b](#)), and  $\gamma$  is the cosine similarity. The scalar  $\lambda$  serves as a balancing factor between the losses; here, we follow the same DualPrompt setting as a baseline.

Table 1: **Performances of Vision Class Incremental Learning (CIL, ViTs)** in terms of Accuracy, Forgetting, Trainable parameters, and Time complexity on 10/20-Split-CIFAR100 and 10-Split-ImageNet-R. Note that Soft-TF performed without FeedForward (FF) networks. \* denotes our reproduced results.

Method	ViT-B/12		10-Split-CIFAR100		20-Split-CIFAR100		10-Split-ImageNet-R	
	#Tr.Params.	Task ID	ACC/Forget	Tr./Test[sec]	ACC/Forget	Tr./Test[sec]	ACC/Forget	Tr./Test[sec]
L2P*	<b>0.03M</b>	Prompt ID	83.77 / 6.63	<b>12.00K / 75</b>	71.29 / 13.96	<b>11.50K / 76</b>	60.44 / 9.00	<b>12.80K / 46</b>
+ PGP*	0.03M	Prompt ID	84.34 / 5.59	12.30K / 75	76.12 / 13.26	12.70K / 76	61.40 / 8.03	13.07K / 46
+ <b>Soft-TF</b> -L[3,4,5]	6.93M	Prompt ID	86.26 / <b>4.79</b>	12.85K / 78	76.17 / 15.77	13.98K / 100	<b>69.80 / 5.13</b>	14.23K / 49
+ <b>Soft-TF</b> -L[10,11,12]	6.93M	<b>Gradient ID</b>	<b>86.46</b> / 4.87	12.87K / 128	<b>77.67</b> / 15.84	13.95K / 160	69.56 / 5.28	14.23K / 79
DualPrompt*	<b>0.03M</b>	Prompt ID	86.50 / 5.77	<b>12.12K / 76</b>	82.98 / 8.20	<b>11.60K / 78</b>	68.13 / 4.46	<b>13.10K / 47</b>
+ PGP*	0.03M	Prompt ID	86.92 / 5.35	<b>12.21K / 76</b>	83.74 / 7.91	<b>13.12K / 78</b>	63.34 / 4.53	<b>13.33K / 47</b>
+ Adapter-L[all], r=75	6.93M	Prompt ID	86.51 / 4.75	14.98K / 90	84.48 / 5.81	16.13K / 109	70.56 / 4.71	15.65K / 54
+ LoRA-L[10,11,12], r=500	6.93M	Prompt ID	82.00 / 4.33	13.24K / 79	92.14 / 2.02	15.89K / 105	43.51 / 13.21	15.09K / 53
+ <b>Soft-TF</b> -L[10,11,12]	6.93M	Prompt ID	<b>92.35</b> / <b>2.98</b>	13.87K / 80	<b>97.40</b> / <b>0.57</b>	15.60K / 104	<b>76.62</b> / <b>5.30</b>	15.35K / 52
+ <b>Soft-TF</b> -L[10,11,12]	6.93M	<b>Gradient ID</b>	<b>98.05</b> / <b>0.25</b>	13.71K / 130	<b>98.96</b> / <b>0.23</b>	15.51K / 163	<b>83.70</b> / <b>0.53</b>	15.08K / 82

## 5 Experiments

We validate our Soft-TF on several benchmark datasets against continuous learning baselines in (1) *Class-Incremental Learning (CIL) based on ViT models*<sup>1</sup> and (2) *CIL based on language models*<sup>2</sup>.

### 5.1 Experimental Settings

**Datasets.** (1) *CL based on ViT models*: we evaluate our method mainly on 1) 10/20-Split-CIFAR100 (Krizhevsky et al., 2009), constructed by splitting the 100 classes into 10 tasks/20 tasks. 2) 10-Split-TinyImageNet (Abai and Rajmalwar, 2019), constructed by splitting the 200 classes into 10 tasks. 3) 10-Split-ImageNet-R (Hendrycks et al., 2021), constructed by splitting the 200 classes into 10 tasks. To show our effectiveness, we additionally compare our method with the baselines on 5-Split-CUB200 and 10-Split-TinyImageNet. (2) *CL based on language models*: we test our method on the widely adopted continual learning benchmarks for language models following de Masson D’Autume et al. (2019), which use five text classification datasets (Chen et al., 2020; Zhang et al., 2015) including AG News (news classification), Yelp (sentiment analysis), DBPedia (Wikipedia article classification), Amazon (sentiment analysis) and Yahoo Answers (Q&A classification).

**Baselines.** To validate the powerfulness of our method in (1) *CL based on ViT models*, we compare our results with various CIL baselines including, L2P (Wang et al., 2022c), DualPrompt (Wang et al., 2022b), and DualPrompt-PGP (Qiao et al., 2024). Moreover, to show the effectiveness of our method in (2) *CL based on language models*, we set MBPA++ (de Masson D’Autume et al., 2019), IDBR (Huang et al., 2021), SLM (Bohao et al., 2024), and DualPrompt (Wang et al., 2022b) as baselines.

Table 2: **Performances of Language Class Incremental Learning (CIL, Bert)** in terms of Accuracy, Forgetting, Trainable parameters, and Time complexity on Bert benchmark datasets. “DR”: data replay. \* denotes our reproduced results.

Method	DR	Task ID	Order: 4 ACC/Forget	Order: 5 ACC/Forget	Order: 6 ACC/Forget	Order: 7 ACC/Forget	Average ACC/Forget	Bert-base (110.0M) #Tr.Params	Tr./Test[sec]
MBPA++	✓	L.Adapter	74.9 / 3.71	73.1 / 2.76	74.9 / 2.89	74.1 / 3.00	74.3 / 3.09	110.0M	30.12K / 87.43
IDBR	✓	L.Adapter	75.9 / 3.46	76.2 / 2.33	76.4 / 2.88	76.7 / 2.90	76.3 / 2.89	110.0M	27.73K / 86.22
SLM*		Retrieval	78.2 / 0.70	77.8 / 0.70	78.0 / 0.70	78.2 / 0.70	78.1 / 0.70	7.32M	17.51K / 73.36
DualPrompt*-L[3,4,5]		Prompt ID	69.7 / 0.02	67.5 / 0.04	69.1 / 0.04	68.8 / 0.03	68.9 / 0.03	<b>0.24M</b>	<b>13.86K / 70.14</b>
DualPrompt*-L[10,11,12]		Prompt ID	67.2 / 0.06	65.1 / 0.09	66.5 / 0.08	66.3 / 0.07	66.3 / 0.08	0.24M	13.86K / 70.14
+ Adapter-L[all], r=16		Prompt ID	75.0 / 0.00	75.1 / 0.00	75.1 / 0.00	75.1 / 0.00	75.1 / 0.00	7.54M	19.45K / 75.34
+ LoRA-L[all], r=96		Prompt ID	78.9 / 0.00	78.9 / 0.00	78.9 / 0.00	78.9 / 0.00	78.9 / 0.00	7.28M	21.57K / 76.61
+ <b>Soft-TF-L[3,4,5]</b> (SOTA)		Prompt ID	79.3 / 0.00	<b>79.6 / 0.00</b>	<b>79.4 / 0.00</b>	79.4 / 0.00	<b>79.4 / 0.00</b>	7.23M	15.51K / 71.12
+ <b>Soft-TF-L[10,11,12]</b>		Prompt ID	<b>79.5 / 0.00</b>	79.3 / 0.00	79.3 / 0.00	<b>79.5 / 0.00</b>	79.4 / 0.00	7.23M	15.53K / 71.12

**Task Inference.** At the inference time, we infer task identity for arbitrary pieces of task samples  $\mathbf{x}$  for finding the proper task nuances and demonstrating full fine-tuning results. We summarize the following two methods:

- **Prompt ID:** For a test example  $\mathbf{x}$ , we simply choose the best matched task index via  $\text{argmin}_t \gamma(q(\mathbf{x}), \mathbf{k}_t)$ .
- **Gradient ID:** To infer the task identity, we follow one-shot task inference. In short, we assign each learned subnetwork  $\mathbf{m}_t$  a weight  $\alpha_t$  such that  $\sum_t \alpha_t = 1$  and  $\alpha_t = 1/\mathcal{T} > 0$  when evaluating all seen tasks. Given an example data point of batch  $\mathbf{x} \in \mathbf{b}$  to classify, we can compute the loss as

1. <https://github.com/ihaeyong/Soft-TF.git>  
2. <https://github.com/ihaeyong/LLM-Soft-TF.git>

$\mathcal{L} = \mathcal{H}(f_{\theta \odot (\sum_t \alpha_t \mathbf{m}_t)}^{prompt}(\mathbf{x}))$  where  $f_{\theta}^{prompt}(\mathbf{x})$  is the pre-trained model which outputs logits and  $\mathcal{H}$  is the entropy function. From here our inferred task is simply  $\hat{t} = \operatorname{argmin}_t \frac{\partial \mathcal{H}}{\partial \alpha_t}$ .

Table 3: **Performances of Vision Class Incremental Learning (CIL, ViTs)** in terms of Pretained-dataset (ImageNet-21K, SAM, DINO) and Task-IDs on 10-Split-CIFAR100 and 5-Split-CUB200.

Method	Pretrained-dataset	Task ID	10-Split-CIFAR100		5-Split-CUB200	
			ACC(†)	Forget(↓)	ACC(†)	Forget(↓)
DualPrompt	ImageNet-21K	Prompt ID	86.50	5.77	82.02	4.23
DualPrompt-PGP	ImageNet-21K	Prompt ID	86.92	5.35	82.46	3.76
DualPrompt	SAM	Prompt ID	86.11	6.08	82.02	4.73
DualPrompt	DINO	Prompt ID	64.18	23.81	50.88	10.10
+Soft-TF	ImageNet-21K	Prompt ID	92.42	2.44	76.17	9.04
+Soft-TF (SOTA)	<b>ImageNet-21K</b>	<b>Gradient ID</b>	<b>97.87</b>	<b>0.21</b>	<b>87.93</b>	<b>0.66</b>
+Soft-TF (SOTA)	<b>SAM</b>	<b>Gradient ID</b>	<b>97.87</b>	<b>0.21</b>	<b>87.93</b>	<b>0.66</b>
+Soft-TF	DINO	Gradient ID	84.50	12.27	69.79	10.93
Upper-Bound of Soft-TF	-	-	93.90	-	85.56	-

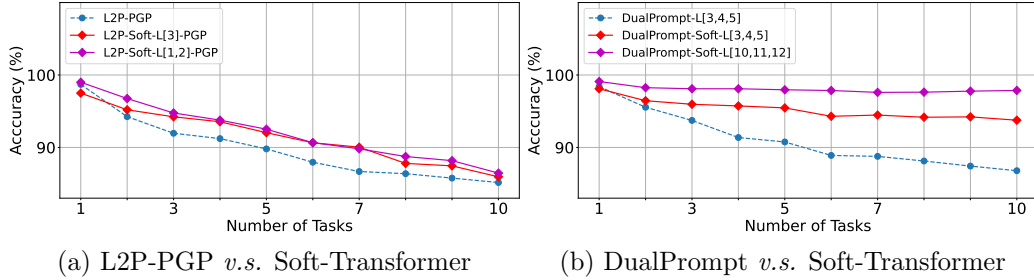


Figure 5: **Layer-wise(L[\*]) Performances of Soft-TF** on 10-Split-CIFAR100. Note that L[9,10,11] denotes Soft-TransFormer of 9, 10, 11 Layers.

## 5.2 Performances

**Performances of Soft-TF on Vision CIL.** We compare our Soft-TransFormers (Soft-TF) with state-of-the-art CIL baselines, as shown in Table 1. Our Soft-TF significantly outperforms all baselines: Adapter and LoRA and upper-bounds of Soft-TF, including L2P and DualPrompt, in accuracy and forgetting measurements. The time complexity of training and testing does not seem to be a significant issue under the same trainable parameters. The performance gain of Soft-TF is especially notable in DualPrompt-based learning compared to L2P, suggesting the importance of global prompt-tuning and multi-head attention prompt-tuning in DualPrompt. Additionally, task-identity inference using Gradient-ID is crucial for achieving full fine-tuning results in CIL.

**Performances of Soft-TF on Language CIL.** Our Soft-TF significantly outperforms all baselines including MBPA++, IDBR, SLM, and DualPrompt in accuracy and forgetting measurements, as shown in Table 2. Replay-based methods, i.e., MBPA++ and IDBR, carry a computational burden since they replay the previous task’s samples and fine-tune 110.0M parameters. SLM shows inefficient time complexity since it takes two stages (warmup and fine-tuning) in the training step and the retrieval process in the inference step. Moreover, Soft-TF performs better than LLM-based fine-tuning baselines such as Adapter and LoRA

under the same trainable parameter settings. Soft-TF trains and tests faster than LLM-based baselines since Soft-TF fine-tunes sparse layers (i.e., [3,4,5] layers). Note that LoRA failed to fine-tune onto sparse [3,4,5] layers.

### 5.3 Ablation Studies

**Well-initialized LTH (WLTH) on Vision CIL.** To demonstrate the efficacy of our proposed method on Well-initialized Lottery Ticket Hypothesis (WLTH) backbones, we evaluate our Soft-TransFormers (Soft-TF) by extending two distinct pre-trained models, ViT-DINO and ViT-SAM (Caron et al., 2021; Chen et al., 2021). As shown in Table 3, we tested our method on the 10-Split-CIFAR100 and 5-Split-CUB200 datasets using three pre-trained ViTs: ImageNet-21K, DINO, and SAM, further validating the effectiveness of our approach on non-ImageNet datasets (Krizhevsky et al., 2009; Wah et al., 2011). Surprisingly, when initialized with ImageNet-21K and SAM, DualPrompt-Soft-TF with ImageNet-21K achieved the same performance levels. Moreover, DualPrompt-Soft-TF outperformed all baselines, i.e., DualPrompt-PGP, on both benchmark datasets, indicating that well-initialized weights provide better generalization in continual learning scenarios.

**Random initialization.** Random initialization of Soft-Transformer’s weights plays a critical role when leveraging well-pretrained models like Vision Transformers (ViTs). The optimal training point is the parameters of a well-pretrained model. Among the initialization methods, Uniform initialization for Soft-Transformer satisfies this requirement effectively. To validate these claims, we analyze the impact of common random initialization methods, including Xavier, Kaiming, Normal, and Uniform Initialization, as shown in Table 4. The results demonstrate that the same well-initialization point leads to independent optimal task performance, particularly with Gradient ID inference. Furthermore, this ablation study strengthens our Soft-TF with state-of-the-art-performances inspired by the Well-initialized Lottery Ticket Hypothesis (WLTH).

Table 4: **Random initialized Performances of Class Incremental Learning (CIL, ViTs)** in terms of accuracy and forgetting on 10-Split-CIFAR100. Note "w/o FF" denotes "Soft fine-tuning without FeedForward (FF)" networks. DualPrompt’s parameters are pretrained on ImageNet-21K.

DualPrompt	Task ID	Random Init.	10-Split-CIFAR100	
			ACC(↑)	Forget(↓)
+Soft-TF-L[10,11,12] w/o FF	Prompt ID	Xavier	90.59	3.85
+Soft-TF-L[10,11,12] w/o FF	Prompt ID	Kaiming	90.72	3.63
+Soft-TF-L[10,11,12] w/o FF	Prompt ID	Normal	90.45	3.78
+Soft-TF-L[10,11,12] w/o FF	Prompt ID	Uniform(1.0, 1.0)	<u>92.35</u>	<u>2.98</u>
+Soft-TF-L[10,11,12] w/o FF	Gradient ID	Uniform(1.0, 1.0)	<b>98.05</b>	<b>0.25</b>
Upper-Bound of Soft-TF			93.90	-

**Layer-wise Inspections.** We analyze the layer-wise performance of Soft-Transformer with respect to L2P and DualPrompt on the 10-Split-CIFAR100 dataset to identify the optimal configurations, as shown in Figure 5. Our observations reveal that the global prompt in DualPrompt influences Soft-Transformer’s performance differently in L2P and DualPrompt settings. In L2P-PGP, the best performance was achieved with Soft-TransFormers applied to the lower layers ((a) L2P-Soft-TF-L[1,2]-PGP), whereas in DualPrompt, the higher layers ((b) DualPrompt-Soft-TF-L[10,11,12]) yielded the best results. Notably, DualPrompt-Soft-

TF-L[10,11,12] without PGP demonstrated impressive performance, achieving almost zero forgetting (0.21). These findings suggest that our approach could significantly enhance the effectiveness of large-scale Transformer models in continual learning scenarios.

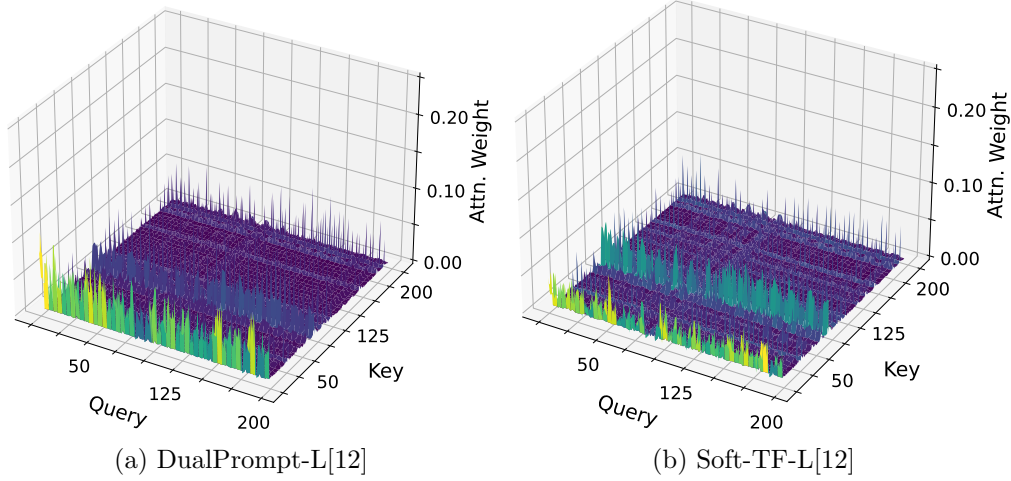


Figure 6: **Attention map comparisons of DualPrompt and Soft-TF**: at Layer-(L[12]) on a single category 7 sample  $x_i^t$  of 10-Split-CIFAR100.

**Attention Layer.** We compare attention maps from the 12th attention layer (L[12]) of two different models, DualPrompt and Soft-TF, applied to category 7 of the 10-Split-CIFAR100 dataset, as shown in Figure 6. While DualPrompt distributes its attention more uniformly, Soft-TF prioritizes specific patches of the input image, likely those more relevant to Category 7. These attention maps highlight the differences in how DualPrompt and Soft-TF allocate attention in a Vision Transformer. Soft-TF’s sharper focus on essential features aligns with the reported superior performance on the 10-Split-CIFAR100 dataset. This visualization emphasizes the interpretability and task-specific optimization of Soft-TF over the more generalized behavior of DualPrompt.

## 6 Conclusion

Inspired by *Well-initialized Lottery Ticket Hypothesis (WLTH)*, which provides suboptimal fine-tuning solutions, we proposed a novel fully fine-tuned continual learning (CL) method referred to as Soft-TransFormers (Soft-TF). Soft-TF sequentially learns and selects an optimal soft-network for each task. During sequential training in CL, an well-initialized Soft-TF mask optimizes the weights of sparse layers to obtain task-adaptive soft (real-valued) networks, while keeping the well-pre-trained layer parameters frozen. In inference, the identified task-adaptive network of Soft-TF masks the parameters of the pre-trained network, mapping to an optimal solution for each task and minimizing Catastrophic Forgetting (CF) - the soft-masking preserves the knowledge of the pre-trained network. Extensive experiments on the Vision Transformer (ViT) and the Language Transformer (Bert) demonstrated the effectiveness of Soft-TF, achieving state-of-the-art performance across Vision and Language CIL scenarios.

## References

- Z. Abai and N. Rajmalwar. Densenet models for tiny imagenet classification. *arXiv preprint arXiv:1904.10429*, 2019. 10
- R. Aljundi, E. Belilovsky, T. Tuytelaars, L. Charlin, M. Caccia, M. Lin, and L. Page-Caccia. Online continual learning with maximal interfered retrieval. In *Advances in Neural Information Processing Systems (NeurIPS)*, 2019. 4
- P. Bohao, Z. Tian, S. Liu, M.-C. Yang, and J. Jia. Scalable language model with generalized continual learning. In *The Twelfth International Conference on Learning Representations*, 2024. 5, 10
- P. Buzzega, M. Boschini, A. Porrello, D. Abati, and S. Calderara. Dark experience for general continual learning: a strong, simple baseline. *Advances in neural information processing systems*, 33:15920–15930, 2020. 4
- L. Caccia, R. Aljundi, N. Asadi, T. Tuytelaars, J. Pineau, and E. Belilovsky. New insights on reducing abrupt representation change in online continual learning. *arXiv preprint arXiv:2104.05025*, 2021. 4
- M. Caron, H. Touvron, I. Misra, H. Jégou, J. Mairal, P. Bojanowski, and A. Joulin. Emerging properties in self-supervised vision transformers. In *Proceedings of the IEEE/CVF international conference on computer vision*, pages 9650–9660, 2021. 12
- A. Chaudhry, M. Ranzato, M. Rohrbach, and M. Elhoseiny. Efficient lifelong learning with a-gem. In *Proceedings of the International Conference on Learning Representations (ICLR)*, 2019a. 2, 4
- A. Chaudhry, M. Rohrbach, M. Elhoseiny, T. Ajanthan, P. K. Dokania, P. H. Torr, and M. Ranzato. Continual learning with tiny episodic memories. *arXiv preprint arXiv:1902.10486*, 2019b. 2, 4
- A. Chaudhry, M. Rohrbach, M. Elhoseiny, T. Ajanthan, P. K. Dokania, P. H. Torr, and M. Ranzato. On tiny episodic memories in continual learning. *arXiv preprint arXiv:1902.10486*, 2019c. 4
- A. Chaudhry, N. Khan, P. K. Dokania, and P. H. Torr. Continual learning in low-rank orthogonal subspaces. In *Advances in Neural Information Processing Systems (NeurIPS)*, 2020. 1, 3
- J. Chen, Z. Yang, and D. Yang. Mixtext: Linguistically-informed interpolation of hidden space for semi-supervised text classification. In *Proceedings of the 58th Annual Meeting of the Association for Computational Linguistics*, pages 2147–2157, 2020. 10
- X. Chen, C.-J. Hsieh, and B. Gong. When vision transformers outperform resnets without pre-training or strong data augmentations. *arXiv preprint arXiv:2106.01548*, 2021. 12
- C. de Masson D’Autume, S. Ruder, L. Kong, and D. Yogatama. Episodic memory in lifelong language learning. *Advances in Neural Information Processing Systems*, 32, 2019. 5, 10



- D. Deng, G. Chen, J. Hao, Q. Wang, and P.-A. Heng. Flattening sharpness for dynamic gradient projection memory benefits continual learning. In *Advances in Neural Information Processing Systems (NeurIPS)*, 2021. 4
- A. Dosovitskiy, L. Beyer, A. Kolesnikov, D. Weissenborn, X. Zhai, T. Unterthiner, M. Dehghani, M. Minderer, G. Heigold, S. Gelly, et al. An image is worth 16x16 words: Transformers for image recognition at scale. *arXiv preprint arXiv:2010.11929*, 2020. 2, 5, 9, 23
- A. Douillard, A. Ramé, G. Couairon, and M. Cord. Dytox: Transformers for continual learning with dynamic token expansion. In *Proceedings of the IEEE/CVF Conference on Computer Vision and Pattern Recognition*, pages 9285–9295, 2022. 2, 5
- D. Hassabis, D. Kumaran, C. Summerfield, and M. Botvinick. Neuroscience-inspired artificial intelligence. *Neuron*, 95(2):245–258, 2017. 1
- D. Hendrycks, S. Basart, N. Mu, S. Kadavath, F. Wang, E. Dorundo, R. Desai, T. Zhu, S. Parajuli, M. Guo, et al. The many faces of robustness: A critical analysis of out-of-distribution generalization. In *Proceedings of the IEEE/CVF international conference on computer vision*, pages 8340–8349, 2021. 10
- N. Houlsby, A. Giurghi, S. Jastrzebski, B. Morrone, Q. De Laroussilhe, A. Gesmundo, M. Attariyan, and S. Gelly. Parameter-efficient transfer learning for nlp. In *International conference on machine learning*, pages 2790–2799. PMLR, 2019. 3, 4, 26
- E. J. Hu, Y. Shen, P. Wallis, Z. Allen-Zhu, Y. Li, S. Wang, L. Wang, and W. Chen. Lora: Low-rank adaptation of large language models. *arXiv preprint arXiv:2106.09685*, 2021. 3, 4, 26
- Y. Huang, Y. Zhang, J. Chen, X. Wang, and D. Yang. Continual learning for text classification with information disentanglement based regularization. *arXiv preprint arXiv:2104.05489*, 2021. 5, 10
- S. Jung, H. Ahn, S. Cha, and T. Moon. Continual learning with node-importance based adaptive group sparse regularization. In *Advances in Neural Information Processing Systems (NeurIPS)*, 2020. 1, 3
- H. Kang, R. J. L. Mina, S. R. H. Madjid, J. Yoon, M. Hasegawa-Johnson, S. J. Hwang, and C. D. Yoo. Forget-free continual learning with winning subnetworks. In *International Conference on Machine Learning*, pages 10734–10750. PMLR, 2022. 2, 4, 23, 24
- H. Kang, J. Yoon, S. R. H. Madjid, S. J. Hwang, and C. D. Yoo. On the soft-subnetwork for few-shot class incremental learning. In *The Eleventh International Conference on Learning Representations*, 2023. URL <https://openreview.net/forum?id=z57WK5lGeHd>. 2, 4, 24
- H. Kang, J. Yoon, S. J. Hwang, and C. D. Yoo. Continual learning: Forget-free winning subnetworks for video representations, 2024a. URL <https://arxiv.org/abs/2312.11973>. 2, 4, 24

- H. Kang, J. Yoon, D. Kim, S. J. Hwang, and C. D. Yoo. Progressive fourier neural representation for sequential video compilation. In *The Twelfth International Conference on Learning Representations*, 2024b. URL <https://openreview.net/forum?id=rGFrRMBb0q>. 4
- M. G. Z. A. Khan, M. F. Naeem, L. Van Gool, D. Stricker, F. Tombari, and M. Z. Afzal. Introducing language guidance in prompt-based continual learning. In *Proceedings of the IEEE/CVF International Conference on Computer Vision*, pages 11463–11473, 2023. 2, 5
- S. Khan, M. Naseer, M. Hayat, S. W. Zamir, F. S. Khan, and M. Shah. Transformers in vision: A survey. *ACM computing surveys (CSUR)*, 54(10s):1–41, 2022. 4
- J. Kirkpatrick, R. Pascanu, N. Rabinowitz, J. Veness, G. Desjardins, A. A. Rusu, K. Milan, J. Quan, T. Ramalho, A. Grabska-Barwinska, et al. Overcoming catastrophic forgetting in neural networks. *Proceedings of the national academy of sciences*, 114(13):3521–3526, 2017. 1, 3
- A. Krizhevsky, G. Hinton, et al. Learning multiple layers of features from tiny images. 2009. 10, 12
- A. Kumar and H. Daume III. Learning task grouping and overlap in multi-task learning. In *Proceedings of the International Conference on Machine Learning (ICML)*, 2012. 3
- X. Li, Y. Zhou, T. Wu, R. Socher, and C. Xiong. Learn to grow: A continual structure learning framework for overcoming catastrophic forgetting. In *Proceedings of the International Conference on Machine Learning (ICML)*, 2019. 2, 4
- X. L. Li and P. Liang. Prefix-tuning: Optimizing continuous prompts for generation. *arXiv preprint arXiv:2101.00190*, 2021. 4
- Z. Li and D. Hoiem. Learning without forgetting. In *Proceedings of the European Conference on Computer Vision (ECCV)*, 2016. 3
- Y.-S. Liang and W.-J. Li. Loss decoupling for task-agnostic continual learning. *Advances in Neural Information Processing Systems*, 36, 2024. 4
- H. Lin, B. Zhang, S. Feng, X. Li, and Y. Ye. Pcr: Proxy-based contrastive replay for online class-incremental continual learning. In *Proceedings of the IEEE/CVF Conference on Computer Vision and Pattern Recognition*, pages 24246–24255, 2023. 4
- Z. Mai, R. Li, H. Kim, and S. Sanner. Supervised contrastive replay: Revisiting the nearest class mean classifier in online class-incremental continual learning. In *Proceedings of the IEEE/CVF Conference on Computer Vision and Pattern Recognition*, pages 3589–3599, 2021. 4
- A. Mallya, D. Davis, and S. Lazebnik. Piggyback: Adapting a single network to multiple tasks by learning to mask weights. In *Proceedings of the European Conference on Computer Vision (ECCV)*, 2018. 2, 4
- M. McCloskey and N. J. Cohen. Catastrophic interference in connectionist networks: The sequential learning problem. In *Psychology of learning and motivation*, volume 24, pages 109–165. Elsevier, 1989. 1, 3

- S. I. Mirzadeh, M. Farajtabar, D. Gorur, R. Pascanu, and H. Ghasemzadeh. Linear mode connectivity in multitask and continual learning. In *Proceedings of the International Conference on Learning Representations (ICLR)*, 2021. 1, 4
- Y. Pei, Z. Qing, S. Zhang, X. Wang, Y. Zhang, D. Zhao, and X. Qian. Space-time prompting for video class-incremental learning. In *Proceedings of the IEEE/CVF International Conference on Computer Vision (ICCV)*, pages 11932–11942, October 2023. 2, 5
- J. Qiao, zhizhong zhang, X. Tan, C. Chen, Y. Qu, Y. Peng, and Y. Xie. Prompt gradient projection for continual learning. In *The Twelfth International Conference on Learning Representations*, 2024. URL <https://openreview.net/forum?id=EH203h7sBI>. 2, 5, 10, 23, 24
- A. Radford, J. W. Kim, C. Hallacy, A. Ramesh, G. Goh, S. Agarwal, G. Sastry, A. Askell, P. Mishkin, J. Clark, et al. Learning transferable visual models from natural language supervision. In *International conference on machine learning*, pages 8748–8763. PMLR, 2021. 2, 5
- A. Razdaibiedina, Y. Mao, R. Hou, M. Khabsa, M. Lewis, and A. Almahairi. Progressive prompts: Continual learning for language models. *arXiv preprint arXiv:2301.12314*, 2023. 4
- S.-A. Rebuffi, A. Kolesnikov, G. Sperl, and C. H. Lampert. icarl: Incremental classifier and representation learning. In *Proceedings of the IEEE conference on Computer Vision and Pattern Recognition*, pages 2001–2010, 2017. 2, 4
- M. Riemer, I. Cases, R. Ajemian, M. Liu, I. Rish, Y. Tu, and G. Tesauro. Learning to learn without forgetting by maximizing transfer and minimizing interference. *arXiv preprint arXiv:1810.11910*, 2018. 2
- A. A. Rusu, N. C. Rabinowitz, G. Desjardins, H. Soyer, J. Kirkpatrick, K. Kavukcuoglu, R. Pascanu, and R. Hadsell. Progressive neural networks. *arXiv preprint arXiv:1606.04671*, 2016. 1, 4
- G. Saha, I. Garg, and K. Roy. Gradient projection memory for continual learning. In *Proceedings of the International Conference on Learning Representations (ICLR)*, 2021. 2, 4
- F. Sarfraz, E. Arani, and B. Zonooz. Error sensitivity modulation based experience replay: Mitigating abrupt representation drift in continual learning. In *The Eleventh International Conference on Learning Representations*, 2023. URL <https://openreview.net/forum?id=zlbci7019Z3>. 4
- J. Serrà, D. Suris, M. Miron, and A. Karatzoglou. Overcoming catastrophic forgetting with hard attention to the task. In *Proceedings of the International Conference on Machine Learning (ICML)*, 2018. 2, 4
- S. Shalev-Shwartz and S. Ben-David. *Understanding machine learning: From theory to algorithms*. Cambridge university press, 2014. 20

- H. Shin, J. K. Lee, J. Kim, and J. Kim. Continual learning with deep generative replay. In *Advances in Neural Information Processing Systems (NeurIPS)*, 2017. 4
- P. Singh, V. K. Verma, P. Mazumder, L. Carin, and P. Rai. Calibrating cnns for lifelong learning. *Advances in Neural Information Processing Systems*, 33:15579–15590, 2020. 4
- J. S. Smith, P. Cascante-Bonilla, A. Arbelle, D. Kim, R. Panda, D. Cox, D. Yang, Z. Kira, R. Feris, and L. Karlinsky. Construct-vl: Data-free continual structured vl concepts learning. In *Proceedings of the IEEE/CVF Conference on Computer Vision and Pattern Recognition (CVPR)*, pages 14994–15004, June 2023a. 2, 5
- J. S. Smith, L. Karlinsky, V. Gutta, P. Cascante-Bonilla, D. Kim, A. Arbelle, R. Panda, R. Feris, and Z. Kira. Coda-prompt: Continual decomposed attention-based prompting for rehearsal-free continual learning. In *Proceedings of the IEEE/CVF Conference on Computer Vision and Pattern Recognition (CVPR)*, pages 11909–11919, June 2023b. 2, 5
- W. Sun, Q. Li, J. Zhang, W. Wang, and Y.-a. Geng. Decoupling learning and remembering: A bilevel memory framework with knowledge projection for task-incremental learning. In *Proceedings of the IEEE/CVF Conference on Computer Vision and Pattern Recognition*, pages 20186–20195, 2023. 4
- S. Thrun. *A Lifelong Learning Perspective for Mobile Robot Control*. Elsevier, 1995. 1, 3
- M. K. Titsias, J. Schwarz, A. G. d. G. Matthews, R. Pascanu, and Y. W. Teh. Functional regularisation for continual learning with gaussian processes. In *Proceedings of the International Conference on Learning Representations (ICLR)*, 2020. 1, 3
- C. Wah, S. Branson, P. Welinder, P. Perona, and S. Belongie. The caltech-ucsd birds-200-2011 dataset. 2011. 12
- Y. Wang, Z. Huang, and X. Hong. S-prompts learning with pre-trained transformers: An occam’s razor for domain incremental learning. *Advances in Neural Information Processing Systems*, 35:5682–5695, 2022a. 2, 5
- Z. Wang, Z. Zhang, S. Ebrahimi, R. Sun, H. Zhang, C.-Y. Lee, X. Ren, G. Su, V. Perot, J. Dy, et al. Dualprompt: Complementary prompting for rehearsal-free continual learning. In *European Conference on Computer Vision*, pages 631–648. Springer, 2022b. 2, 4, 5, 8, 9, 10, 23
- Z. Wang, Z. Zhang, C.-Y. Lee, H. Zhang, R. Sun, X. Ren, G. Su, V. Perot, J. Dy, and T. Pfister. Learning to prompt for continual learning. In *Proceedings of the IEEE/CVF Conference on Computer Vision and Pattern Recognition*, pages 139–149, 2022c. 2, 4, 5, 10, 23
- M. Wortsman, V. Ramanujan, R. Liu, A. Kembhavi, M. Rastegari, J. Yosinski, and A. Farhadi. Supermasks in superposition. In *Advances in Neural Information Processing Systems (NeurIPS)*, 2020. 2, 4, 24
- J. Xu and Z. Zhu. Reinforced continual learning. In *Advances in Neural Information Processing Systems (NeurIPS)*, 2018. 4

- S. Yan, J. Xie, and X. He. Der: Dynamically expandable representation for class incremental learning. In *Proceedings of the IEEE/CVF Conference on Computer Vision and Pattern Recognition*, pages 3014–3023, 2021. 4
- F. Zenke, B. Poole, and S. Ganguli. Continual learning through synaptic intelligence. In *International Conference on Machine Learning*, pages 3987–3995. PMLR, 2017. 1
- X. Zhang, J. Zhao, and Y. LeCun. Character-level convolutional networks for text classification. *Advances in neural information processing systems*, 28, 2015. 10

## Appendix A. Appendix

### A.1 Analysis of Soft-TransFormers (Soft-TF)

**Analysis of Soft-TransFormers for Convex-Lipschitz Functions.** To analyze the convergence rate of the Soft-TransFormers (Soft-TF), we limit ourselves to the case of convex-Lipschitz functions along with the analysis (Shalev-Shwartz and Ben-David, 2014). Let  $\mathbf{w}^* = \{\mathbf{g}^*, \mathbf{e}_t^*, \mathbf{m}_t^*\}$  be any vector or an optimal solution and let  $B$  be an upper bound on  $\|\mathbf{w}^*\|$  when  $\mathbf{w}^{(1)} = \mathbf{0}$ . It is convenient to think of  $\mathbf{w}^*$  as the minimizer of  $f(\mathbf{w})$ , but the analysis that follows holds for every  $\mathbf{w}^*$ .

We obtain an upper bound on the sub-optimality of our solution with respect to  $\mathbf{w}^*$ , namely,  $f(\bar{\mathbf{w}}) - f(\mathbf{w}^*)$ , where  $\bar{\mathbf{w}} = \frac{1}{T}\mathbf{w}^{(t)}$ . From the definition of  $\bar{\mathbf{w}}$ , and using Jensen's inequality, we have that

$$\begin{aligned} f(\bar{\mathbf{w}}) - f(\mathbf{w}^*) &= f\left(\frac{1}{T} \sum_{t=1}^T \mathbf{w}^{(t)}\right) - f(\mathbf{w}^*) \\ &\leq \frac{1}{T} \sum_{t=1}^T \left(f(\mathbf{w}^{(t)}) - f(\mathbf{w}^*)\right) \\ &= \frac{1}{T} \sum_{t=1}^T \left(f(\mathbf{w}^{(t)}) - f(\mathbf{w}^*)\right). \end{aligned} \quad (8)$$

For every  $t$ , because of the convexity of  $f$ , we have that

$$f(\mathbf{w}^{(t)}) - f(\mathbf{w}^*) \leq \left\langle \mathbf{w}^{(t)} - \mathbf{w}^*, \nabla f(\mathbf{w}^{(t)}) \right\rangle \quad (9)$$

Combining the preceeding we obtain

$$f(\mathbf{w}^{(t)}) - f(\mathbf{w}^*) \leq \frac{1}{T} \sum_{t=1}^T \left\langle \mathbf{w}^{(t)} - \mathbf{w}^*, \nabla f(\mathbf{w}^{(t)}) \right\rangle \quad (10)$$

To bound the right-hand side we rely on the following lemma:

**Lemma 1.** *Let  $\mathbf{v}_1, \dots, \mathbf{v}_T$  be an arbitrary sequence of vectors. Any algorithm with an well initialization (pre-trained model)  $\mathbf{w}^{(1)} \neq \mathbf{0}$  and an update rule of the form*

$$\mathbf{w}^{(t+1)} = \mathbf{w}^{(t)} - \eta \mathbf{v}_t \quad (11)$$

*satisfies with  $\|\mathbf{w}^{(1)} - \mathbf{w}^*\|^2 = \|\mathbf{w}^{(T+1)} - \mathbf{w}^*\|^2$*

$$\begin{aligned} \sum_{t=1}^T \left\langle \mathbf{w}^{(t)} - \mathbf{w}^*, \mathbf{v}_t \right\rangle &\leq \frac{1}{2\eta} \|\mathbf{w}_m^{(T+1)} - \mathbf{w}^*\|^2 + \frac{\eta}{2} \sum_{t=1}^T \|\mathbf{v}_t\|^2 \\ &< \frac{1}{2\eta} \|\mathbf{w}_p^{(T+1)} - \mathbf{w}^*\|^2 + \frac{\eta}{2} \sum_{t=1}^T \|\mathbf{v}_t\|^2 \\ &< \frac{1}{2\eta} \|\mathbf{w}^{(T+1)} - \mathbf{w}^*\|^2 + \frac{\eta}{2} \sum_{t=1}^T \|\mathbf{v}_t\|^2 \end{aligned} \quad (12)$$



where  $\mathbf{w}_m \neq \mathbf{w}_q$  since  $\mathbf{m}$  is learnable parameters in Soft-TransFormers. Specifically, we could assume that  $\mathbf{w}_m = (\mathbf{w}^Q \odot \mathbf{m}^Q) \cdot \mathbf{x} \mathbf{p}^T \cdot (\mathbf{w}^K \odot \mathbf{m}^K)^T$  and  $\mathbf{w}_p = (\mathbf{w}^Q \odot \mathbf{1}^Q) \cdot \mathbf{x} \mathbf{p}^T \cdot (\mathbf{w}^K \odot \mathbf{1}^K)^T$  of Equation 6.

**Theorem 2.** For every  $B_m < B_p < B, \rho > 0$  where  $B_m = \|\mathbf{w}_m^{(T+1)} - \mathbf{w}^*\|$  and  $B_p = \|\mathbf{w}_p^{(T+1)} - \mathbf{w}^*\|$ , if for all  $t$  we have that  $\|\mathbf{v}_t\| \leq \rho$  and if we set  $\eta = \sqrt{\frac{B^2}{\rho^2 T}}$ , then for every  $\mathbf{w}^*$  with  $\|\mathbf{w}^{(T+1)} - \mathbf{w}^*\| \leq B$  we have

$$\frac{1}{T} \sum_{t=1}^T \langle \mathbf{w}^{(t)} - \mathbf{w}^*, \mathbf{v}_t \rangle \leq \frac{B_m \rho}{\sqrt{T}} < \frac{B_p \rho}{\sqrt{T}} < \frac{B \rho}{\sqrt{T}}. \quad (13)$$

**Proof** Using algebraic manipulations (completing the square), we obtain:

$$\begin{aligned} & \langle \mathbf{w}^{(t)} - \mathbf{w}^*, \mathbf{v}_t \rangle \\ &= \frac{1}{\eta} \langle \mathbf{w}^{(t)} - \mathbf{w}^*, \eta \mathbf{v}_t \rangle \\ &= \frac{1}{2\eta} \left( -\|\mathbf{w}^{(t)} - \mathbf{w}^* - \eta \mathbf{v}_t\|^2 + \|\mathbf{w}^{(t)} - \mathbf{w}^*\|^2 + \eta^2 \|\mathbf{v}_t\|^2 \right) \\ &= \frac{1}{2\eta} \left( -\|\mathbf{w}^{(t+1)} - \eta \mathbf{v}_t\|^2 + \|\mathbf{w}^{(t)} - \mathbf{w}^*\|^2 \right) + \frac{\eta}{2} \|\mathbf{v}_t\|^2, \end{aligned} \quad (14)$$

where the last equality follows from the definition of the update rule. Summing the equality over  $t$ , we have

$$\begin{aligned} & \sum_{t=1}^T \langle \mathbf{w}^{(t)} - \mathbf{w}^*, \mathbf{v}_t \rangle \\ &= \frac{1}{2\eta} \sum_{t=1}^T \left( -\|\mathbf{w}^{(t+1)} - \eta \mathbf{v}_t\|^2 + \|\mathbf{w}^{(t)} - \mathbf{w}^*\|^2 \right) + \frac{\eta}{2} \sum_{t=1}^T \|\mathbf{v}_t\|^2 \end{aligned} \quad (15)$$

The first sum on the right-hand side is a telescopic sum that collapses to

$$\|\mathbf{w}^{(1)} - \mathbf{w}^*\|^2 = \|\mathbf{w}^{(T+1)} - \mathbf{w}^*\|^2 \quad (16)$$

Plugging this in Equation, we have

$$\begin{aligned} & \sum_{t=1}^T \langle \mathbf{w}^{(t)} - \mathbf{w}^*, \mathbf{v}_t \rangle \\ &= \frac{1}{2\eta} \sum_{t=1}^T \left( -\|\mathbf{w}^{(t+1)} - \eta \mathbf{v}_t\|^2 + \|\mathbf{w}^{(t)} - \mathbf{w}^*\|^2 \right) + \frac{\eta}{2} \sum_{t=1}^T \|\mathbf{v}_t\|^2 \\ &\leq \frac{1}{2\eta} \|\mathbf{w}^{(1)} - \mathbf{w}^*\|^2 + \frac{\eta}{2} \sum_{t=1}^T \|\mathbf{v}_t\|^2 \\ &= \frac{1}{2\eta} \|\mathbf{w}^*\|^2 + \frac{\eta}{2} \sum_{t=1}^T \|\mathbf{v}_t\|^2, \end{aligned} \quad (17)$$

where the last equality is due to the definition  $\mathbf{w}^{(1)} = \mathbf{0}$ . This proves the first part of the lemma. The second part follows by upper bounding  $\|\mathbf{w}\|$  by  $B$ ,  $\|\mathbf{v}_t\|$  by  $\rho$ , deciding by  $T$ , and plugging in the value of  $\eta$ .

In terms of Soft-TransFormers  $\mathbf{w}_m = (\mathbf{w}^Q \odot \mathbf{m}^Q) \cdot \mathbf{x}\mathbf{p}^T \cdot (\mathbf{w}^K \odot \mathbf{m}^K)^T$  of Equation 6, we have

$$\begin{aligned} & \sum_{t=1}^T \langle \mathbf{w}^{(t)} - \mathbf{w}^*, \mathbf{v}_t^s \rangle \\ &= \frac{1}{2\eta} \sum_{t=1}^T \left( -\|\mathbf{w}^{(t+1)} - \eta \mathbf{w}_t\|^2 + \|\mathbf{w}^{(t)} - \mathbf{w}^*\|^2 \right) + \frac{\eta}{2} \sum_{t=1}^T \|\mathbf{v}_t\|^2 \\ &\leq \frac{1}{2\eta} \|\mathbf{w}^{(1)} - \mathbf{w}^*\|^2 + \frac{\eta}{2} \sum_{t=1}^t \|\mathbf{v}_t\|^2 \end{aligned} \quad (18)$$

where  $\mathbf{v}_t$  is an arbitrary  $t$ -th vector and  $\mathbf{w}^{(1)} \neq \mathbf{0}$  since  $\mathbf{w}^Q$  and  $\mathbf{q}^K$  are pre-trained parameters.

however, in term of prompt  $\mathbf{w}_p = (\mathbf{w}^Q \odot \mathbf{1}^Q) \cdot \mathbf{x}\mathbf{p}^T \cdot (\mathbf{w}^K \odot \mathbf{1}^K)^T$ , we have

$$\begin{aligned} & \sum_{t=1}^T \langle \mathbf{w}^{(t)} - \mathbf{w}^*, \mathbf{v}_t^p \rangle \\ &= \frac{1}{2\eta} \sum_{t=1}^T \left( -\|\mathbf{w}^{(t+1)} - \eta \mathbf{w}_t\|^2 + \|\mathbf{w}^{(t)} - \mathbf{w}^*\|^2 \right) + \frac{\eta}{2} \sum_{t=1}^T \|\mathbf{v}_t\|^2 \\ &\leq \frac{1}{2\eta} \|\mathbf{w}^{(1)} - \mathbf{w}^*\|^2 + \frac{\eta}{2} \sum_{t=1}^t \|\mathbf{v}_t\|^2 \end{aligned} \quad (19)$$

where  $\mathbf{v}_t$  is an arbitrary  $t$ -th vector of prompt and  $\mathbf{w}^{(1)} \neq \mathbf{0}$  since  $(\mathbf{w} \odot \mathbf{1})^Q$  and  $(\mathbf{w} \odot \mathbf{1})^K$  are pre-trained parameters,  $\mathbf{w}^Q$  and  $\mathbf{w}^K$ , respectively.

Therefore, we have from  $\|\mathbf{w}^{(1)} - \mathbf{w}^*\|^2 = \|\mathbf{w}^{(T+1)} - \mathbf{w}^*\|^2$

$$\begin{aligned} & \sum_{t=1}^T \langle \mathbf{w}^{(t)} - \mathbf{w}^*, \mathbf{v}_t^p \rangle \\ &\leq \frac{1}{2\eta_m} \|\mathbf{w}_m^{(T+1)} - \mathbf{w}^*\|^2 + \frac{\eta_m}{2} \sum_{t=1}^t \|\mathbf{v}_t\|^2 \\ &< \frac{1}{2\eta_p} \|\mathbf{w}_p^{(T+1)} - \mathbf{w}^*\|^2 + \frac{\eta_p}{2} \sum_{t=1}^t \|\mathbf{v}_t\|^2 \\ &< \frac{1}{2\eta} \|\mathbf{w}^{(T+1)} - \mathbf{w}^*\|^2 + \frac{\eta}{2} \sum_{t=1}^T \|\mathbf{v}_t\|^2 \end{aligned} \quad (20)$$

where  $\|\mathbf{w}_m^{(1)} - \mathbf{w}^*\|^2 < \|\mathbf{w}_p^{(1)} - \mathbf{w}^*\|^2$  since all  $\mathbf{m}$  are learnable parameters.

For every  $B_m < B_p < B, \rho > 0$  where  $B_m = \|\mathbf{w}_m^{(T+1)} - \mathbf{w}^*\|$  and  $B_p = \|\mathbf{w}_p^{(T+1)} - \mathbf{w}^*\|$ , if for all  $t$  we have that  $\|\mathbf{v}_t\| \leq \rho$  and if we set  $\eta \approx \eta_m \approx \eta_p = \sqrt{\frac{B^2}{\rho^2 T}}$  with large enough  $T$ , then for every  $\mathbf{w}^*$  with  $\|\mathbf{w}^{(T+1)} - \mathbf{w}^*\| \leq B$  we have

$$\frac{1}{T} \sum_{t=1}^T \langle \mathbf{w}^{(t)} - \mathbf{w}^*, \mathbf{v}_t \rangle \leq \frac{B_m \rho}{\sqrt{T}} < \frac{B_p \rho}{\sqrt{T}} < \frac{B \rho}{\sqrt{T}}. \quad (21)$$

■

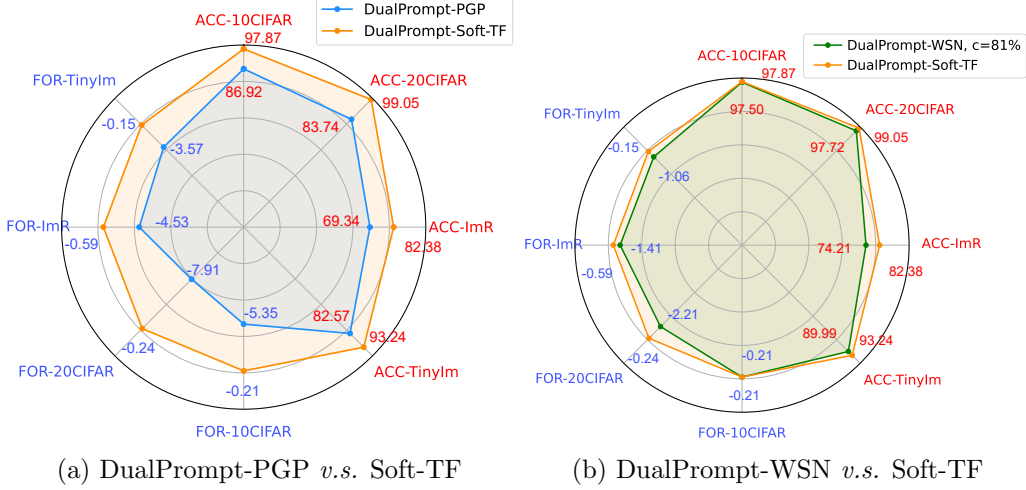


Figure 7: **Radar Chart of Comparisons** in terms of average accuracy and forgetting between baselines and our SOTA method (Soft-TF). DualPrompt-PGP (Qiao et al., 2024) and DualPrompt-WSN (Kang et al., 2022) (c% sparsity) are baselines for prompt tuning and subnetworks. ACC refers to the average accuracy metric (higher is better). FOR refers to the forgetting metric (lower is better). Different scale standards are adopted for two metrics on benchmark datasets.

## A.2 Experimental Details

For fair comparisons with the baselines (Wang et al., 2022c,b; Qiao et al., 2024), we use ViT B/16 (Dosovitskiy et al., 2020) pre-trained on ImageNet-21K as our image encoder, which is kept frozen during training. We train and test on a single Quadro RTX 8000-48GB GPU for baselines and our Soft-TransFormers with Adam optimizer with  $\beta_1 = 0.9$  and  $\beta_2 = 0.999$ .

We adhere to the experimental settings outlined by Qiao et al. (2024) to validate our method’s effectiveness. When comparing our approach with L2P-PGP and Soft-Transformer on the 10/20-Split-CIFAR100 and 10-Split-TinyImageNet datasets, we train the network for 5 epochs with a batch size of 16 and set the prompt length to 5. For the 10-Split-ImageNet-R dataset, we use 50 epochs, a batch size of 16, and a prompt length of 30. In comparison with DualPrompt-PGP and Soft-TransFormers on the 10/20-Split-CIFAR100 dataset, we train the network for 20 epochs with a batch size of 24 and set the expert prompt length to 5. For the 10-Split-TinyImageNet dataset, we use 5 epochs, a batch size of 24, and an expert prompt length of 5. For the 10-Split-ImageNet-R dataset, we set the epochs to 50, the batch size to 24, and the expert prompt length to 20. Additionally, in all benchmark data sets, the

general prompt length is set to 5, and the location inserted into the prompt is kept consistent.

**CLIP on CIL and TIL.** We conduct our experiments on the 10-Split-CIFAR100 dataset under both Class Incremental Learning (CIL) and Task Incremental Learning (TIL) settings, as shown in Table 5. The results demonstrate that CLIP-Prompt-Soft-TF-L[1-12] significantly improves performance in both settings, indicating that our Soft-TF with Gradient ID is also effective in vision-language models, thereby broadening its applicability.

Table 5: **Comparisons of Soft-TF with baselines based on CLIP model** on 10-Split-CIFAR100. \* denotes our reproduced results.

Method	Task ID	Class Incremental		Task Incremental	
		ACC(↑)	Forget(↓)	ACC(↑)	Forget(↓)
CLIP	Prompt ID	73.76	5.60	92.69	2.34
CLIP-PGP	Prompt ID	79.47	4.23	93.00	1.58
CLIP*	Prompt ID	74.60	7.75	93.59	2.80
CLIP-PGP*	Prompt ID	74.63	7.76	93.67	2.83
CLIP-Prompt	Prompt ID	70.27	12.95	93.36	3.07
CLIP-Prompt-Soft-TF-L[3,4,5]	Prompt ID	71.58	7.73	95.29	1.12
CLIP-Prompt-Soft-TF-L[3,4,5]	Gradient ID	76.77	5.59	95.29	1.12
CLIP-Prompt-Soft-TF-L[1-12]	Prompt ID	72.28	3.44	96.83	0.44
CLIP-Prompt-Soft-TF-L[1-12] (SOTA)	Gradient ID	<b>85.90</b>	<b>3.07</b>	<b>96.83</b>	<b>0.44</b>

For CLIP-PGP and Soft-TransFormers, we configure a single trainable image prompt that is shared across all tasks within the vision encoder. For the text encoder, following the approach of Qiao et al. (2024), we set a trainable text prompt for each class, which is only trained on the corresponding task. In our comparisons with CLIP-PGP and Soft-TransFormers on the 10-Split-CIFAR100 dataset, we set the image prompt length to 5, the number of epochs to 5, and the batch size to 32.

**Training & Test Time.** To clearly illustrate the time complexity of Soft-TF, we present the training and testing times for 10/20-Split-CIFAR100 and 10-Split-ImageNet-R, as shown in Table 7. As the number of trainable parameters in Soft-TF increases, training and testing time complexities grow accordingly. While the testing time complexity of Gradient ID increased by approximately 1.6 times across the three benchmark datasets, it consistently improved task performance on all benchmarks. The corresponding performance metrics are detailed in Table 8. We also investigate the most parameter-efficient and gradient-based task inference methods, as shown in Table 9 and Table 10. Our findings reveal that the 3-shot Gradient ID inference cost (using samples within a mini-batch) with the last layer (Soft-TF-L[12]) is approximately 1.1 times that of Prompt ID, maintaining comparable efficiency while delivering superior performance. Note that m-batch denotes mini-batch.

**Soft & Subnetworks** have been explored in continual learning through the following notable approaches such as supermasks (Wortsman et al., 2020), WSN (Kang et al., 2022), SoftNet (Kang et al., 2023), and FSO (Kang et al., 2024a). All prior works have primarily demonstrated the effectiveness of sparse solutions in fully connected networks and Convolutional Neural Networks (CNNs). Sparse fine-tuning mechanisms have not been investigated for pre-trained transformers, such as ViT, and remain unexplored. To discover the competitive sparseness in Transformers, we detail the WSN-style task-adaptive fine-tuning and

Table 6: **Performances of Class Incremental Learning (CIL)** in terms of accuracy and forgetting on 10/20-Split-CIFAR100 and 10-Split-ImageNet-R. Exemplar means the total buffer size for rehearsal methods.

Method	Exemplar	Task ID	10-Split-CIFAR100		20-Split-CIFAR100		10-Split-ImageNet-R	
			ACC( $\uparrow$ )	Forget( $\downarrow$ )	ACC( $\uparrow$ )	Forget( $\downarrow$ )	ACC( $\uparrow$ )	Forget( $\downarrow$ )
BiC	5,000	-	81.42	17.31	73.02	6.23	64.63	22.25
DER++	5,000	-	83.94	14.55	-	-	66.73	20.67
iCaRL	5,000	-	66.00	5.33	78.02	5.80	-	-
DER+MCG	2,000	-	67.62	14.64	65.84	13.72	-	-
BiC	1,000	-	66.11	35.24	63.12	21.89	52.14	36.70
DER++	1,000	-	61.06	39.87	-	-	55.47	34.64
iCaRL	1,000	-	61.25	14.19	71.32	15.98	-	-
FT	-	-	33.61	86.87	33.52	53.69	28.87	63.80
EWC	-	-	47.01	33.27	36.73	35.19	35.00	56.16
LWF	-	-	60.69	27.77	39.12	57.91	38.54	52.37
L2P*	-	Prompt ID	83.77	6.63	71.29	13.96	60.44	9.00
L2P-PGP*	-	Prompt ID	84.34	5.59	76.12	<b>13.26</b>	61.40	8.03
L2P-PGP-Soft-TF	-	Prompt ID	86.26	<b>4.79</b>	76.17	15.77	<b>69.80</b>	<b>5.13</b>
L2P-PGP-Soft-TF	-	Gradient ID	<b>86.46</b>	4.87	<b>77.67</b>	15.84	69.56	5.28
DualPrompt	-	Prompt ID	86.50	5.77	82.98	8.20	68.13	4.46
DualPrompt-Soft-TF-L[3,4,5]	-	Prompt ID	91.77	3.37	94.43	2.02	74.70	6.46
DualPrompt-Soft-TF-L[3,4,5]	-	Gradient ID	93.76	1.83	95.38	1.73	82.15	2.20
DualPrompt-WSN-L[10,11,12], c=80.0 %	-	Gradient ID	97.41	0.18	90.25	9.08	74.83	0.91
DualPrompt-WSN-L[10,11,12], c=81.0 %	-	Gradient ID	97.50	0.21	96.72	2.21	74.21	1.41
DualPrompt-WSN-L[10,11,12], c=82.0 %	-	Gradient ID	97.67	0.27	96.44	1.62	75.02	0.92
DualPrompt-WSN-L[10,11,12], c=87.0 %	-	Gradient ID	97.51	0.27	97.68	0.75	77.96	1.02
DualPrompt-WSN-L[10,11,12], c=90.0 %	-	Gradient ID	97.46	0.38	98.09	0.65	78.80	0.47
DualPrompt-Soft-TF-L[10,11,12]	-	Gradient ID	<b>97.87</b>	<b>0.21</b>	<b>99.05</b>	<b>0.24</b>	<b>82.38</b>	<b>0.59</b>
DualPrompt-PGP	-	Prompt ID	86.92	5.35	83.74	7.91	69.34	4.53
DualPrompt-PGP-Soft-TF-L[3,4,5]	-	Prompt ID	92.41	2.44	95.14	1.90	74.65	4.39
DualPrompt-PGP-Soft-TF-L[3,4,5]	-	Gradient ID	<b>92.92</b>	<b>2.34</b>	<b>95.89</b>	<b>1.64</b>	<b>81.45</b>	<b>2.89</b>
Upper-Bound of DualPrompt	-	-	90.85	-	90.85	-	79.13	-
Upper-Bound of Soft-TF	-	-	93.90	-	93.90	-	80.21	-

 Table 7: **Performances of Class Incremental Learning (CIL)** in terms of **Soft parameters, training, and test time** on 10/20-Split-CIFAR100 and 10-Split-ImageNet-R. Note "w/o FF" denotes "Soft finetuning without FeedForward (FF)" networks.

Method	ViT-B/12 (85.8M) # Train Params.	Task ID	10-Split-CIFAR100		20-Split-CIFAR100		10-Split-ImageNet-R	
			Train (sec.)	Test (sec.)	Train (sec.)	Test (sec.)	Train (sec.)	Test (sec.)
DualPrompt	0.03M	Prompt ID	12.12K	76	11.60K	78	13.10K	47
PGP	0.03M	Prompt ID	12.21K	76	13.12K	78	13.33K	47
Soft-TF-L[12] w/ only ATTN	1.76M	Gradient ID	12.18K	129	13.30K	113	13.35K	65
Soft-TF-L[12] w/ only ATTN	1.76M	Prompt ID	12.18K	78	13.30K	80	13.35K	48
Soft-TF-L[12] w/o FF	2.31M	Gradient ID	12.24K	103	13.40K	132	13.42K	66
Soft-TF-L[11,12] w/o FF	4.62M	Gradient ID	12.95K	115	14.38K	146	14.23K	73
Soft-TF-L[10,11,12] w/o FF	6.93M	Gradient ID	13.71K	130	15.51K	163	15.08K	82
Soft-TF-L[10,11,12] w/o FF	<u>6.93M</u>	<u>Prompt ID</u>	<u>13.87K</u>	<u>80</u>	<u>15.60K</u>	<u>104</u>	<u>15.35K</u>	<u>52</u>
LoRA-L[10,11,12] w/o FF, r=4	0.06M	Prompt ID	11.95K	77	11.71K	79	14.34K	48
LoRA-L[10,11,12] w/o FF, r=24	0.32M	Prompt ID	12.03K	78	15.10K	100	15.02K	50
LoRA-L[10,11,12] w/o FF, r=500	<u>6.93M</u>	<u>Prompt ID</u>	<u>13.24K</u>	<u>79</u>	<u>15.89K</u>	<u>105</u>	<u>15.09K</u>	<u>53</u>
Adapter-L[10,11,12] w/ FF, r=1	0.09M	Prompt ID	12.44K	84	12.40K	81	14.40K	50
Adapter-L[10,11,12] w/ FF, r=4	0.36M	Prompt ID	12.80K	85	15.35K	105	14.68K	51
Adapter-L[10,11,12] w/ FF, r=300	<u>6.93M</u>	<u>Prompt ID</u>	<u>13.66K</u>	<u>88</u>	<u>15.72K</u>	<u>106</u>	<u>15.50K</u>	<u>53</u>

the learnable soft-networks ***m*** of Transformers, presenting these adaptations for the first time with empirical observations. Here, the Soft-TF originates from learned parameters distributed with  $\mu \approx 1.0$  & various variances, as stated in Figure 3: we observed that each task solution has its unique variances which help infer task-ID in gradient step. To demonstrate the effectiveness of Soft-TF, Figure 7(a) presents a radar chart comparing

Table 8: **Performances of Class Incremental Learning (CIL)** in terms of **Soft parameters, Accuracy, and Forget** on 10/20-Split-CIFAR100 and 10-Split-ImageNet-R. Note "w/o FF" denotes "Soft finetuning without FeedForward (FF)" networks.

Method	ViT-B/12 (85.8M)		10-Split-CIFAR100	20-Split-CIFAR100	10-Split-ImageNet-R			
DualPrompt	# Train Params.	Task ID	ACC(↑)	Forget(↓)	ACC(↑)	Forget(↓)	ACC(↑)	Forget(↓)
DualPrompt	0.03M	Prompt ID	86.50	5.77	82.98	8.20	68.13	4.46
PGP	0.03M	Prompt ID	86.92	5.35	83.74	7.91	69.34	4.53
Soft-TF-L[12] w/ only ATTN	1.76M	Gradient ID	97.17	0.40	98.09	0.54	72.31	3.94
Soft-TF-L[12] w/ only ATTN	1.76M	Prompt ID	94.59	1.12	96.96	1.02	71.13	4.93
Soft-TF-L[12] w/o FF	2.31M	Gradient ID	96.84	0.55	97.81	0.57	81.18	1.31
Soft-TF-L[11,12] w/o FF	4.62M	Gradient ID	97.58	0.34	98.65	0.43	83.09	0.42
Soft-TF-L[10,11,12] w/o FF	6.93M	Gradient ID	98.05	0.25	98.96	0.23	<b>83.70</b>	<b>0.53</b>
Soft-TF-L[10,11,12] w/o FF	<u>6.93M</u>	<u>Prompt ID</u>	<u>92.35</u>	<u>2.98</u>	<u>97.40</u>	<u>0.57</u>	<u>76.62</u>	<u>5.30</u>
LoRA-L[10,11,12] w/o FF, r=4	0.06M	Prompt ID	82.19	4.33	93.74	2.07	70.91	9.11
LoRA-L[10,11,12] w/o FF, r=24	0.32M	Prompt ID	86.77	4.27	95.65	1.04	69.81	10.30
LoRA-L[10,11,12] w/o FF, r=500	<u>6.93M</u>	<u>Prompt ID</u>	<u>82.00</u>	<u>4.33</u>	<u>92.14</u>	<u>2.02</u>	<u>43.51</u>	<u>13.21</u>
Adapter-L[10,11,12] w/ FF, r=1	0.09M	Prompt ID	86.38	4.87	85.61	5.04	70.95	4.31
Adapter-L[10,11,12] w/ FF, r=4	0.36M	Prompt ID	86.53	4.52	85.66	5.00	70.82	4.90
Adapter-L[10,11,12] w/ FF, r=300	<u>6.93M</u>	<u>Prompt ID</u>	<u>86.45</u>	<u>4.61</u>	<u>84.75</u>	<u>5.11</u>	<u>70.55</u>	<u>4.74</u>

Table 9: **Performances of Class Incremental Learning (CIL)** in terms of **Soft parameters, training, and test time** on 10/20-Split-CIFAR100 and 10-Split-ImageNet-R. Note "w/o FF" denotes "Soft finetuning without FeedForward (FF)" networks.

Method	ViT-B/12 (85.8M)		10-Split-CIFAR100		20-Split-CIFAR100		10-Split-ImageNet-R	
DualPrompt	# Train Params.	Task ID	Train (sec.)	Test (sec.)	Train (sec.)	Test (sec.)	Train (sec.)	Test (sec.)
DualPrompt	0.03M	Prompt ID	12.12K	76	11.60K	78	13.10K	47
PGP	0.03M	Prompt ID	12.21K	76	13.12K	78	13.33K	47
Soft-TF-L[12] w/o FF	2.31M	Prompt ID	12.24K	79	13.40K	80	13.42K	48
Soft-TF-L[12] w/o FF	2.31M	Gradient ID, 3-shot	<u>12.24K</u>	<u>88</u>	<u>13.40K</u>	<u>90</u>	<u>13.42K</u>	<u>57</u>
Soft-TF-L[12] w/o FF	2.31M	Gradient ID, 5-shot	12.24K	94	13.40K	98	13.42K	61
Soft-TF-L[12] w/o FF	2.31M	Gradient ID, 7-shot	12.24K	95	13.40K	108	13.42K	62
Soft-TF-L[12] w/o FF	2.31M	Gradient ID, m-batch	12.24K	103	13.40K	132	13.42K	66
Soft-TF-L[10,11,12] w/o FF	6.93M	Prompt ID	13.87K	<u>80</u>	15.60K	104	15.35K	52
Soft-TF-L[10,11,12] w/o FF	6.93M	Gradient ID, 3-shot	13.71K	96	15.51K	106	15.08K	63
Soft-TF-L[10,11,12] w/o FF	6.93M	Gradient ID, 5-shot	13.71K	96	15.51K	109	15.08K	74
Soft-TF-L[10,11,12] w/o FF	6.93M	Gradient ID, 7-shot	13.71K	106	15.51K	119	15.08K	75
Soft-TF-L[10,11,12] w/o FF	6.93M	Gradient ID, batch	13.71K	130	15.51K	163	15.08K	82

DualPrompt-PGP and Soft-TransFormers across four benchmark datasets with various sparseness (Figure 7(b) & Table 6.): we compare the performance of DualPrompt-WSN and Soft-TF using accuracy across tasks on the 10-Split CIFAR100 dataset. The performances of Soft-TF provide the upper bound of WSN, as shown in Figure 8(a). In Vision Transformers, Figure 8(b) demonstrates the existences of a smooth solution of SoftNet.

**Comparisons of Soft-TF with LLMs.** To demonstrate the effectiveness of Soft-TF, we compare Soft-TF against LLM fine-tuning methods such as Adapters (Houlsby et al., 2019) and LoRA (Hu et al., 2021), as shown in Table 8. Under identical experimental conditions—including trainable model parameters (6.9M per task), layers (L[10,11,12]), and Prompt ID—Soft-TF outperformed other LLM-based fine-tuning approaches. The results highlight that directly updating well-pretrained model parameters and prompt-tuning via Soft-TF is more effective than combining representations through LoRA or learning representations with Adapters. Furthermore, we observed that Soft-TF and the other methods exhibited comparable training and testing time complexity for the same number of trainable parameters. Notably, single-layer fine-tuning using Soft-TF (with L[12]) surpasses



Table 10: **Performances of Class Incremental Learning (CIL)** in terms of **Soft parameters, Accuracy, and Forget** on 10/20-Split-CIFAR100 and 10-Split-ImageNet-R. Note "w/o FF" denotes "Soft finetuning without FeedForward (FF)" networks.

Method	ViT-B/12 (85.8M)		10-Split-CIFAR100	20-Split-CIFAR100	10-Split-ImageNet-R			
DualPrompt	# Train Params.	Task ID	ACC(↑)	Forget(↓)	ACC(↑)	Forget(↓)		
DualPrompt	0.03M	Prompt ID	86.50	5.77	82.98	8.20	68.13	4.46
PGP	0.03M	Prompt ID	86.92	5.35	83.74	7.91	69.34	4.53
Soft-TF-L[12] w/o FF	2.31M	Prompt ID	91.83	2.99	96.43	1.00	72.45	5.32
Soft-TF-L[12] w/o FF	2.31M	Gradient ID, 3-shot	93.12	1.82	96.43	1.00	73.55	4.80
Soft-TF-L[12] w/o FF	2.31M	Gradient ID, 5-shot	96.13	0.58	96.43	1.00	75.04	4.49
Soft-TF-L[12] w/o FF	2.31M	Gradient ID, 7-shot	96.51	0.65	96.43	1.00	76.34	4.75
Soft-TF-L[12] w/o FF	2.31M	Gradient ID, batch	96.84	0.55	97.81	0.57	81.18	1.31
Soft-TF-L[10,11,12] w/o FF	6.93M	Prompt ID	92.35	2.98	97.40	0.57	74.62	5.30
Soft-TF-L[10,11,12] w/o FF	6.93M	Gradient ID, 3-shot	93.92	1.62	97.40	0.57	74.99	4.21
Soft-TF-L[10,11,12] w/o FF	6.93M	Gradient ID, 5-shot	97.37	0.53	97.40	0.57	77.40	2.91
Soft-TF-L[10,11,12] w/o FF	6.93M	Gradient ID, 7-shot	97.76	0.51	97.40	0.57	79.33	3.57
Soft-TF-L[10,11,12] w/o FF	6.93M	Gradient ID, m-batch	98.05	0.25	98.96	0.23	83.70	0.53

the performance of the baselines. These findings firmly establish Soft-TF as the most competitive approach among strong LLM baselines (Adapters and LoRA) in the continual learning (CIL) scenario.

**Sparsity of Transformer.** We inspect the sparse solution through WSN as shown in Table 6, Table 11, and Table 12. We found a suboptimal sparse solution ( $c=87.0\%$  on 10-Split-TinyImageNet) with minimal CF through the inspections, as stated in Table 11. This demonstrates the Lottery Ticket Hypothesis (LTH) in transformers, a competitive sparse subnetwork in DenseNetwork. In addition, DualPrompt is the lower-bound while DualPrompt-Soft-TF-\* is the upper-bound, close to the optimal performances.

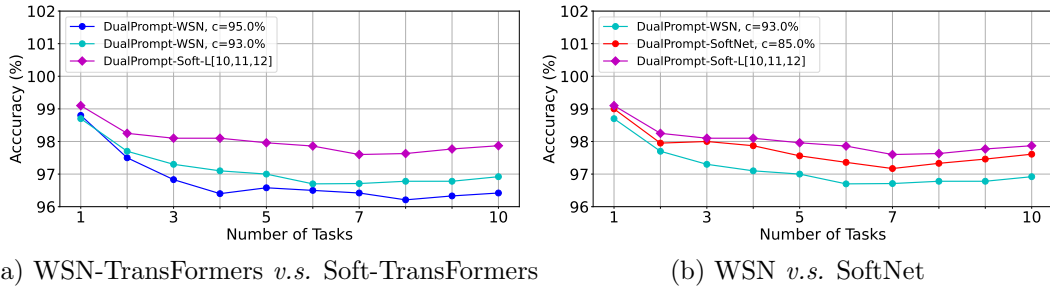


Figure 8: **Comparisons of Soft-Transformers with Subnetworks** on 10-Split-CIFAR100. Note that L[10,11,12] denotes the fine-tuning layers of 10, 11, and 12.

**Pseudo Codes.** The overall process of the Soft-Transformers (Soft-TF) during training and testing is described as Algorithm 1 and Algorithm 2. We denote the architecture with attached prompts as  $f_{g,e_t,m_t}$ . The input  $\mathbf{x}$  from the  $t$ -th task is transformed using  $f_{g,e_t,m_t}$  and then passed to the classification head  $f_\phi$ , parameterized by  $\phi$ , for prediction. Finally, we train the two prompts, the task keys, the soft-attention parameters, and the newly-initialized classification head in an end-to-end manner.

**Density of Parameters.** We inspect the histogram density estimate of the last (12) layer's parameters of DualPrompt-Soft-TF: attention of QKV ((a) ATTN.QKV) and Projection ((b) ATTN.PROJ) and multi-layer perception (MLP) of FC1 and FC2, as shown in Figure 9.

Table 11: **Performances of Subnetworks (WSN) in Class Incremental Learning (CIL) on 10-Split-TinyImageNet.**

Method	Pretrained-Dataset	Task ID	TinyImageNet	
			ACC( $\uparrow$ )	Forget( $\downarrow$ )
DualPrompt	-	Prompt ID	86.50	5.77
DualPrompt-WSN-L[10,11,12]	C=80.0%	Gradient ID	89.95	0.98
DualPrompt-WSN-L[10,11,12]	C=81.0%	Gradient ID	89.99	1.06
DualPrompt-WSN-L[10,11,12]	C=82.0%	Gradient ID	89.59	1.18
DualPrompt-WSN-L[10,11,12]	C=83.0%	Gradient ID	90.60	0.72
DualPrompt-WSN-L[10,11,12]	C=85.0%	Gradient ID	90.09	1.07
DualPrompt-WSN-L[10,11,12]	C=87.0%	Gradient ID	<u>91.91</u>	<u>0.38</u>
DualPrompt-WSN-L[10,11,12]	C=90.0%	Gradient ID	91.28	0.42
DualPrompt-WSN-L[10,11,12]	C=93.0%	Gradient ID	91.41	0.40
DualPrompt-WSN-L[10,11,12]	C=95.0%	Gradient ID	90.91	0.83
DualPrompt-Soft-TF-L[10,11,12]	-	Gradient ID	<b>97.87</b>	<b>0.21</b>

Table 12: **Performances of Class Incremental Learning (CIL) in terms of Soft parameters, Accuracy, and Forget on 10/20-Split-CIFAR100 and 10-Split-ImageNet-R.** Note "w/ only ATTN" denotes "Soft finetuning only with attention (ATTN)" and FeedForward (FF) networks.

Method DualPrompt	ViT-B/12 (85.8M) #Tr. Params.	Task ID	10-Split-CIFAR100		20-Split-CIFAR100		10-Split-ImageNet-R	
			ACC	Forget	ACC	Forget	ACC	Forget
DualPrompt	0.03M	Prompt ID	86.50	5.77	82.98	8.20	68.13	4.46
<b>PGP</b>	0.03M	Prompt ID	86.92	5.35	83.74	7.91	69.34	4.53
<b>Soft-TF-L</b> [12] w/ only ATTN	1.76M	Gradient ID	97.17	0.40	98.09	0.54	72.31	3.94
<b>Soft-TF-L</b> [12] w/ only ATTN, c=90%	<b>1.58M</b>	Gradient ID	96.81	0.61	97.51	1.68	71.67	3.94

ATTN’s QKV parameters have the largest variance among the parameter densities, while MLP-FC2’s are the smallest. From this observation, we conclude that fine-tuning ATTN’s QKV is required to achieve optimal task performance. In other words, QKV’s parameters are more critical than others.

**Pre-trained Parameters vs. Soft-TF.** We inspect the histogram density estimate of the last (12) layer’s parameters of pre-trained model and DualPrompt-Soft-TF: attention of QKV ((a) ATTN.QKV) and Projection ((b) ATTN.PROJ) and multi-layer perception (MLP) of FC1 and FC2, as shown in [Figure 10](#). The most parameters of DualPrompt-Soft-TF are trained around zero-values. Particularly, the difference between pre-trained model’s parameters and Soft-TF is distinctive at QKV module.

---

**Algorithm 1** DualPrompt-Soft-TF at training time
 

---

```

1: Input: Pre-trained transformer-based backbone  $f$ , final classification layer  $f_\phi$ ,
2:   number of tasks  $\mathcal{T}$ , training set  $\{\{\mathbf{x}_{i,t}, y_{i,t}\}_{i=1}^{n_t}\}_{t=1}^{\mathcal{T}}$ , G-Prompt  $\mathbf{g}$ , E-Prompt  $\mathbf{E} = \{\mathbf{e}_t\}_{t=1}^{\mathcal{T}}$ ,
3:   task keys  $\mathbf{K} = \{\mathbf{k}_t\}_{t=1}^{\mathcal{T}}$ , soft-networks  $\mathbf{M} = \{\mathbf{m}_t\}_{t=1}^{\mathcal{T}}$ ,  $start_g, end_g, start_e, end_e$ ,
4:   prompting function  $f_{\theta \odot \mathbf{m}}^{prompt}$ ,
5:   number of training epochs of the  $t$ -th task  $\mathcal{K}_t$ .
6: Initialize:  $\phi, \mathbf{g}, \mathbf{E}, \mathbf{M}, \mathbf{K}$ 
7: for task  $t = 1, \dots, \mathcal{T}$  do
8:   Select the task-specific E-Prompt, soft-network  $\mathbf{e}_t, \mathbf{m}_t$  and corresponding task key  $\mathbf{k}_t$ 
9:   Generate the prompted architecture  $f_{\mathbf{g}, \mathbf{e}_t, \mathbf{m}_t}$ : attach  $\mathbf{g}$  and  $\mathbf{e}_t$  to  $start_g$ -th to  $end_g$ -th
10:    and  $start_e$ -th to  $end_e$ -th soft MSA layers respectively, with  $f_{\theta \odot \mathbf{m}}^{prompt}$ .
11:   for batch  $\mathbf{e}_s \sim \mathcal{K}_t$  do
12:     Draw a mini-batch  $B = \{(\mathbf{x}_{i,t}, y_{i,t})\}_{i=1}^l$ 
13:     for  $(\mathbf{x}, y)$  in  $B$  do
14:       Calculate the prompted feature by
15:       Calculate the per sample loss  $\mathcal{L}_x$  via
16:     end for
17:     Update  $\phi, \mathbf{g}, \mathbf{E}, \mathbf{M}, \mathbf{K}$  by back-propagation
18:   end for
19: end for
    
```

---



---

**Algorithm 2** DualPrompt-Soft-TF at test time
 

---

```

1: Given components: Pre-trained transformer-based backbone  $f$ , trained
2:    $\mathbf{K} = \{\mathbf{k}_t\}_{t=1}^{\mathcal{T}}, \mathbf{M} = \{\mathbf{m}_t\}_{t=1}^{\mathcal{T}}, start_g, end_g, start_e, end_e$ , prompting function  $f_{\theta \odot \mathbf{m}}^{prompt}$ 
3: Input: test example  $\mathbf{x}$  from mini-batch  $\mathbf{b}$ 
4: Select task inference method: (1) Prompt ID or (2) Gradient ID
5:   (1) Prompt ID:
6:     Generate query feature  $q(\mathbf{x})$ 
7:     Matching for the index of E-Prompt via  $t_{\mathbf{x}} = \operatorname{argmin}_t \gamma(q(\mathbf{x}), \mathbf{k}_t)$ 
8:   (2) Gradient ID:
9:     Assigning each learned subnetwork  $\mathbf{m}_t$  a weight  $\alpha_t$  such that  $\sum_t \alpha_t = 1$  and  $\alpha_t = 1/\mathcal{T} > 0$ .
10:    Given  $\mathbf{x} \in \mathbf{b}$  to classify, we can compute our loss  $\mathcal{L} = \mathcal{H}(f_{\theta \odot (\sum_t \alpha_t \mathbf{m}_t)}^{prompt}(\mathbf{x}))$ 
11:    Matching for the index of E-Prompt via  $t_{\mathbf{x}} = \operatorname{argmin}_t \frac{\partial \mathcal{H}}{\partial \alpha_t}$ 
12:   Select the task-specific E-prompt  $\mathbf{e}_{t_{\mathbf{x}}}$  and learned subnetwork  $\mathbf{m}_{t_{\mathbf{x}}}$ 
13:   Generate the prompted architecture  $f_{\mathbf{g}, \mathbf{e}_{t_{\mathbf{x}}}, \mathbf{m}_{t_{\mathbf{x}}}}$ :
14:     Attaching  $\mathbf{g}$  and  $\mathbf{e}_{t_{\mathbf{x}}}$  to  $start_g$ -th to  $end_g$ -th
15:     and  $start_e$ -th to  $end_e$ -th MSA layers respectively, with  $f_{\theta \odot \mathbf{m}}^{prompt}$ .
16: Prediction:  $f_{\mathbf{g}, \mathbf{e}_{t_{\mathbf{x}}}, \mathbf{m}_{t_{\mathbf{x}}}}(\mathbf{x})$ 
    
```

---

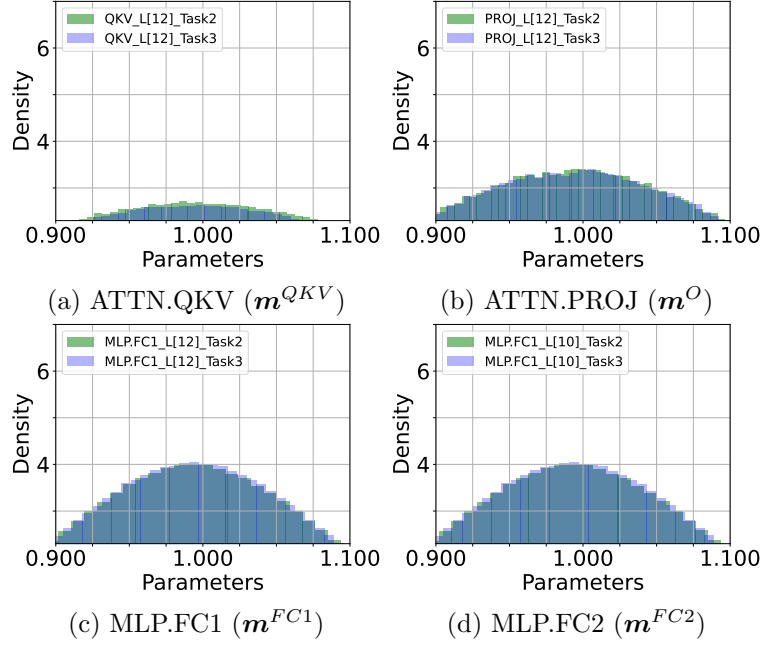


Figure 9: **Layer-(L[12]) Histogram Density Estimates of DualPrompt-Soft-TF's Parameters** on 10-Split-CIFAR100.

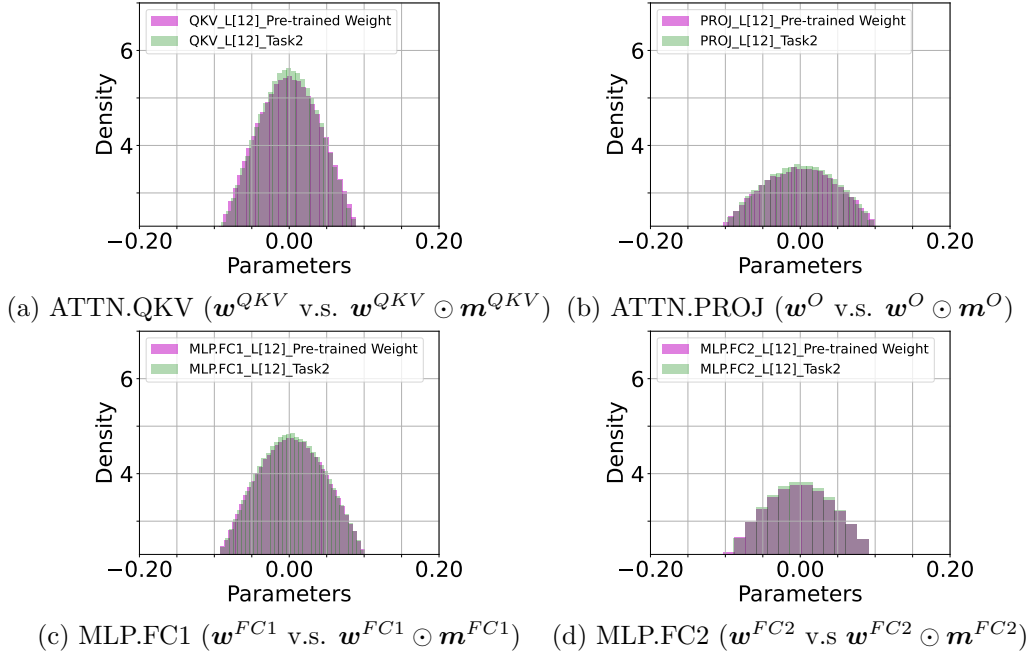


Figure 10: **Layer-(L[12]) Histogram Density Estimates of Pre-trained Weight and DualPrompt-Soft-TF's Parameters** on 10-Split-CIFAR100.